

# Extension to the Delimara Power Station: IPPC Permit

*Our ref: ENV33019/A/10*

*Your ref: EPD/A/RD/10/283*

**Consolidated Version  
Addendum 2**

## **PREDICTION OF THE SPREAD AND DILUTION OF COOLING WATER FROM DELIMARA POWER STATION**

*August 2011*



**ais** environmental ltd.

AIS House, 18 St. John Street, Fgura FGR 1447 – MALTA

Tel: +356 21803374 Fax: +356 21803434

Website: [www.aisenvironmental.com](http://www.aisenvironmental.com)



global environmental solutions

**Delimara Power Station, Malta**

**Prediction of the Spread and Dilution of Cooling Water from  
Delimara Power Station**

SLR Ref  
August 2011



## CONTENTS

<b>0.0 EXECUTIVE SUMMARY .....</b>	<b>1</b>
<b>1.0 INTRODUCTION.....</b>	<b>4</b>
1.1 Quality Assurance.....	4
<b>2.0 STUDY AREA AND INPUTS.....</b>	<b>5</b>
2.1 Study Area .....	5
2.2 DPS Operations .....	5
2.3 Environmental Sensitivity.....	6
<b>3.0 MATHEMATICAL MODEL .....</b>	<b>7</b>
3.1 Model Set-Up .....	7
3.2 Water Depth Data .....	9
3.3 Water Movement.....	10
3.4 Temperature.....	10
<b>4.0 MODEL RESULTS .....</b>	<b>12</b>
4.1 Tidal Influences Waves & Winds.....	12
4.2 Tidal plus Mediterranean Sea Circulation .....	21
4.3 Tidal, Circulation and Seiche effects.....	24
<b>5.0 ENVIRONMENTAL IMPACT .....</b>	<b>27</b>
5.1 Sensitive Receptors .....	27
5.2 Ecological Effects of Warm Water Discharge.....	27
<b>6.0 CONCLUSIONS.....</b>	<b>29</b>
<b>7.0 CLOSURE.....</b>	<b>30</b>

## TABLES

<b>Table 1 Harmonic Constants for Water Elevation.....</b>	<b>12</b>
--	-----------

## FIGURES

<b>Figure 1 Google Earth image showing the Delimara Power Station (DPS) .....</b>	<b>5</b>
<b>Figure 2 Admiralty Chart Extract of DPS Outfall.....</b>	<b>5</b>
<b>Figure 3 Mathematical Model Area.....</b>	<b>7</b>
<b>Figure 4 Model Grid - Overview .....</b>	<b>8</b>
<b>Figure 5 Model Grid – Detail of DPS Intake &amp; Outfall .....</b>	<b>8</b>
<b>Figure 6 Water Depths (m) to Chart datum: Model overview.....</b>	<b>9</b>
<b>Figure 7 Water depths (m) Chart datum: at DPS.....</b>	<b>10</b>
<b>Figure 8 Measured Sea Water Temperatures at Mellieha-Bay, Malta.....</b>	<b>11</b>
<b>Figure 9 Tidal Elevations (cm) for 22/9/2011 to 10/10/2011 (hours).....</b>	<b>13</b>
<b>Figure 10 Tidal Flow Marsaxlokk inlet: No Discharge Flood Tide (top) &amp; Ebb Tide (bottom).....</b>	<b>14</b>
<b>Figure 11 Tidal Flows in il Hofra iz Zghira: No Discharge Flood Tide (top) &amp; Ebb Tide (bottom).....</b>	<b>15</b>
<b>Figure 12 Flows in il Hofra iz Zghira: Existing DPS Discharge.....</b>	<b>16</b>
<b>Figure 13 DPS Existing Discharge Winter Conditions: Surface temperatures (left) &amp; Seabed temperatures (right) .....</b>	<b>17</b>
<b>Figure 14 DPS Existing Discharge Winter Conditions with Significant Wave Action: Surface temperatures (left) &amp; Seabed temperatures (right) .....</b>	<b>17</b>
<b>Figure 15 DPS Existing Discharge Winter Conditions: North-West wind 10 m/s (left), North-East 10 m/s wind (right) .....</b>	<b>18</b>
<b>Figure 16 DPS Existing Discharge Summer Conditions: Surface temperatures (left) &amp; Seabed temperatures (right) .....</b>	<b>19</b>
<b>Figure 17 DPS Increased Discharge Winter Conditions: Surface temperatures (left) &amp; Seabed temperatures (right) .....</b>	<b>20</b>

<b>Figure 18 DPS Increased Discharge Winter Conditions &amp; significant wave action: Surface temperatures (left) &amp; Seabed temperatures (right) .....</b>	<b>20</b>
<b>Figure 19 DPS Increased Discharge Summer Conditions: Surface temperatures (left) &amp; Seabed temperatures (right) .....</b>	<b>21</b>
<b>Figure 20 Mediterranean Sea General Water Circulation for June.....</b>	<b>22</b>
<b>Figure 21 General Circulation Surface Flows for September by Sorgente et al. (2003).....</b>	<b>22</b>
<b>Figure 22 Tidal plus Circulation Flows in the Surface Waters near DPS.....</b>	<b>23</b>
<b>Figure 23 DPS Winter Conditions temperature for tidal plus circulation flows: Existing Discharge (left), Increased Discharge (right).....</b>	<b>24</b>
<b>Figure 24 Tidal Heights, Grand Harbour, Valletta (23/24th June 2011) .....</b>	<b>25</b>
<b>Figure 25 Tidal heights, Marsaxlokk Bay: 2009 (top), detail (bottom).....</b>	<b>25</b>
<b>Figure 26 DPS Winter Conditions: Tidal, Circulation and Seiche flows: Existing Discharge (left), Increased Discharge (right).....</b>	<b>26</b>

## **APPENDICES**

### **Appendix A FVCOM MODEL**

## **DRAWINGS**

### **Drawing 1 Environmentally Sensitive Areas**

## 0.0 EXECUTIVE SUMMARY

This report describes the results of mathematical modelling of the Delimara Power Station (DPS) cooling water discharge into the bay, il Hofra iz Zghira, in the south-east of Malta.

The model predicts temperatures in the coastal waters from the present DPS cooling water discharge and has been used to simulate the effects of an increase in the heated water discharge arising from an increase in the generating capacity of the DPS.

The FVCOM model has been used to model the cooling water discharge from DPS. Data to set-up and validate the model have been gathered from sources such as Admiralty Charts, Tide Tables, Transport Malta, published meteorological data, and technical publications describing the annual variation in sea water temperature and water circulation around Malta.

Modelling is an effective tool for comparing the impact of different discharge scenarios for giving a good insight into expected effects. Results indicate good correlation though specific data to validate the model are limited.

Modelling considers the effects of tides, water circulation, seiches, wind and wave action on the movement, spread and dilution of the DPS cooling water plume. Without the discharge flows in il Hofra iz Zghira, where the discharge is situated, are very low (~1 cm/s). Flows in the Bay increase offshore to approximately 15 cm/s.

DPS cooling water discharges are an existing flow rate of 29,500 m<sup>3</sup>/h and for an increased capacity to 43,000 m<sup>3</sup>/h; both at 8°C above the ambient water temperature.

Results indicate that:-

Flows generated by the DPS discharge dominate the circulation in the bay but merge into the coastal flow within 500 m offshore from the mouth of the bay.

Predicted temperature contours have the same characteristics in winter and summer (summer temperatures are seasonally higher). Results are most easily described in terms of a) increases above the ambient temperature of the coastal waters; and b) the difference between the temperature of the sea surface and the sea bed.

### Existing discharge rate:

- Surface temperature in the coastal waters (i.e. outside of il Hofra iz Zghira bay) are up to 1.5°C above background, and the temperature at the mouth of the bay is +2°C. Within the bay temperatures increase to +8°C at the outfall with the highest temperatures along the west and north coasts.
- Sea bed temperatures outside the bay are unaffected by the discharge. Within the bay sea bed temperatures are increased along the western and northern shores.
- Under conditions of strong winds and wave action the vertical mixing in the area is increased resulting in warmer water being mixed to the sea bed. Water of +0.5°C is predicted to occur at the bed in limited areas outside the bay; the sea bed temperature at the southern point of the mouth of the bay is +1°C, which would give a maximum of 28°C at the height of the summer.

### Increased discharge rate:

- Surface temperature in the coastal waters (i.e. outside of il Hofra iz Zghira bay) are up to 2°C above background, and the temperature at the mouth of the bay on the

northern side is +3°C. Within the bay temperatures increase to +8°C at the outfall with the highest temperatures along the west and north coasts.

- Sea bed temperatures outside the bay are unaffected by the discharge. Within the bay sea bed temperatures are increased along the western and northern shores.
- Under conditions of strong winds and wave action the vertical mixing in the area is increased resulting in warmer water being mixed to the sea bed. Water of +1°C is predicted to occur at the bed in limited areas outside the bay, and the sea bed temperature at the southern point of the mouth of the bay is +1.5°C in a very small area, which would give a maximum of 28.5°C at the height of the summer.

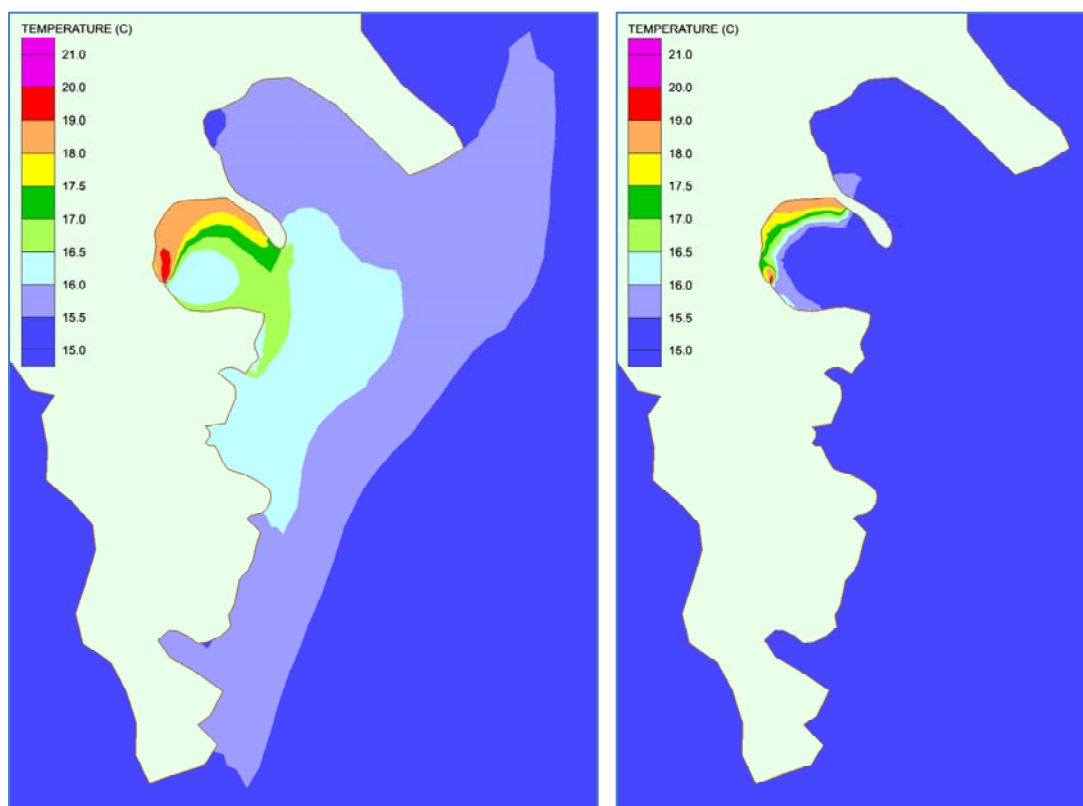
#### Effects on Noble Pen Shell, *Pinna nobilis*

Existing cooling water discharges and an increase in capacity is highly unlikely to have an effect on the populations that are known to exist.

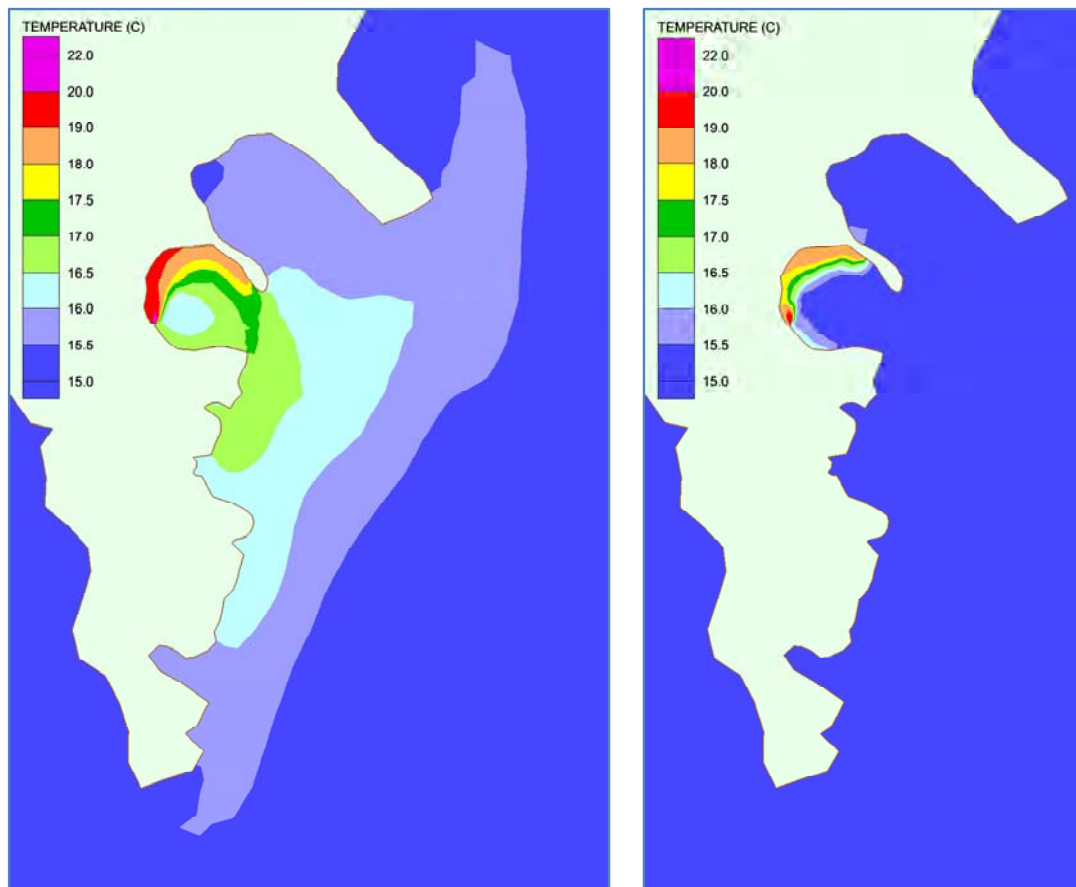
Outside il Hofra iz Zghira and at the habitat locations identified as being mostly likely to be affected, predicted peak summer temperatures are within the normal range for these organisms. No significant effect on habitat or population is likely.

Within il Hofra iz Zghira bay, moderate increases in sea bed water temperature would not act as a barrier to populations existing in these areas. Insufficient data exists to determine whether there is the potential to restrict spawning or recruitment within the bay, but it is considered unlikely that any effect would have a discernable limiting effect on existing populations.

#### **Existing - Surface (left) & Sea bed (right) Temperature: Winter Condition**



**Future - Surface (left) & Sea bed (right) Temperature: Winter Condition**



## **1.0 INTRODUCTION**

Development to increase the capacity of the Delimara Power Station (DPS) will result in additional cooling water discharges. This report describes the set-up of the mathematical model to predict the movement and dispersion of the heated water from DPS discharge. The model has been used to predict the existing warm water plume in the coastal zone and the size of the plume if the discharge is increased.

AIS Environmental Limited (AIS) provides engineering, planning and environmental support to the Delimara Project. AIS are supported by SLR Consulting for technical environmental assessment including the impact of cooling water releases. SLR has commissioned a mathematical model of the area to predict the spread and dispersion of the cooling water in the local coastal waters.

The modelling study aims to predict the areas where the temperature of the coastal waters are raised by 0.5°C or more above the ambient water temperature for the current discharge and for the proposed increase in the discharge. Predictions are used to assess the vulnerability of ecologically sensitive areas in the coastal waters adjacent to the discharge.

Modelling considers the effects of:-

- Before DPS - No Cooling Water Discharge
- Existing DPS - Cooling Water Discharge
- Future DPS - Cooling Water Discharge

Appendix A provides the detailed modelling on which this assessment is based.

### **1.1 Quality Assurance**

SLR Consulting is accredited to ISO 9001 quality management system to ensure work to the highest standards. All work is completed within standard operating procedures and recognised national and international guidelines.



## 2.0 STUDY AREA AND INPUTS

### 2.1 Study Area

Figure 1 shows the DPS on the peninsula, between Marsaxlokk Bay and the bay, il Hofra iz Zghira. Figure 2 gives the admiralty chart extract showing the specific location of the intake and discharge. Water is extracted from Marsaxlokk bay on the left hand side of the images and discharged on the opposite side of the peninsula into il Hofra iz Zghira to the right.

**Figure 1 Google Earth image showing the Delimara Power Station (DPS)**



Google Earth image, July 2011.

**Figure 2 Admiralty Chart Extract of DPS Outfall**



1© Crown Copyright and/or database rights. Reproduced by permission of the Controller of Her Majesty's Stationery Office & UK Hydrographic Office([www.ukho.gov.uk](http://www.ukho.gov.uk))H and Seapro. Licence number 14835. Not to be used for navigation.

### 2.2 DPS Operations

#### Existing Operations

The DPS complex houses 295MW of generating capacity.

Existing cooling water discharge is 29,500 m<sup>3</sup>/h (8.194 m<sup>3</sup>/s). The temperature is 8°C above the temperature of the coastal waters.

#### Increased Capacity

The proposed increase generating capacity is 144MW to 439MW.

This will result in an additional 13,500m<sup>3</sup>/hr cooling water flow to a total of 43,000 m<sup>3</sup>/h (11.944 m<sup>3</sup>/s). Discharge temperature will remain as 8°C above ambient.

## Outfall

The outfall is located on the shoreline in on the south-west edge of il Hofra iz Zghira.

It is constructed of reinforced concrete and discharges just below the mean low water level - protruding no more than 10-15m into the sea.

It comprises a twin, box-section, culvert approximately 3.5m in width (1.75m ea). Each half is provided with a penstock valve and coarse screen with lockable access.

### **2.3 Environmental Sensitivity**

The discharge and il Hofra iz Zghira is not within a Special Area of Conservation. However, there are records of potentially sensitive marine habitat areas nearby.

The nearest potentially sensitive area is located at the mouth of il Hofra iz Zghira and is almost directly east at ~374m at its nearest point. This records *P oceanica* meadows with low densities of *Pinna nobilis*. The majority of this habitat is over 500m from the outfall. The nearest records of high density are more than 1km distant.

Environmental records (Drawing 1) show sea bed habitat (meadows) of the seagrass, Neptune Grass or Mediterranean tapeweed. Three areas in which *Pinna nobilis* are found nearby are (Tahht-il-Maqjel, Ras il Friek, Ras-il-Qali). Of these two (Ras il Friek and Ras il Qali) are found at the mouth of il Hofra iz Zghira bay.

These meadows support the protected Noble Pen Shell, *Pinna nobilis* [also referred to as the fan mussel]. *P. nobilis* is listed as endangered under the 1992 European Council Directive on the conservation of natural habitats and wild fauna and flora (92/43/EEC, Annex IV). It has been protected by the Protocol for Specially Protected Areas Biological Diversity in the Mediterranean (Barcelona Convention: UNEP).

Section 5.2 provides additional information on *Pinna nobilis* and the impact of cooling water discharges from the existing and future situation.

### 3.0 MATHEMATICAL MODEL

The Finite Volume Coastal Ocean Model (FVCOM) used for this study is a 3-dimensional hydrodynamic model to compute tidal flows and temperature variations in estuaries, coastal regions or in the open ocean. It was created at the Marine Ecosystem Dynamics Modelling Laboratory in the School of Marine Science and Technology at the University of Massachusetts-Dartmouth<sup>1</sup>. In this study FVCOM has been applied to the central area of the Mediterranean Sea with the specific aim to predict the movement and dispersion of the cooling water discharged from DPS located at the eastern end of Malta.

Appendix A gives additional information about FVCOM.

#### 3.1 Model Set-Up

Figure 3 show the extent of the model area (extent shown by dashed white lines) covering the central area of the Mediterranean Sea from northern Tunisia & Libya to Sicily.

**Figure 3 Mathematical Model Area**



Image from Google Earth, 27/7/2011

The grid becomes more refined as the islands of Malta are approached and is detailed (3m grid) around the DPS water intake and the cooling water discharge.

<sup>1</sup> Chen C, Liu H, R C Beardsley R C, 2003. An unstructured, finite-volume, three-dimensional, primitive equation ocean model: application to coastal ocean and estuaries. (<http://fvcom.smast.umassd.edu/FVCOM/index.html>).



A triangular grid pattern (Figure 4) is used in the computation of the tidal flows. The grid varies from large triangles (~30 km) in the west and becomes more refined as the islands of Malta are approached. Figure 5 shows the detail of the area and the model grid around DPS including the positions of the water intake and the cooling water discharge. The finest part of the model grid is at the outfall, where the grid triangles expand from a minimum of 3 m to 15 m in the area of the discharged cooling water plume.

The quality of the triangles across the whole model grid is controlled so that the minimum interior angle is greater than  $30^\circ$  and the maximum angle is  $130^\circ$ . The maximum change in area between adjacent triangles is controlled to be less than a factor of 2.

**Figure 4 Model Grid - Overview**

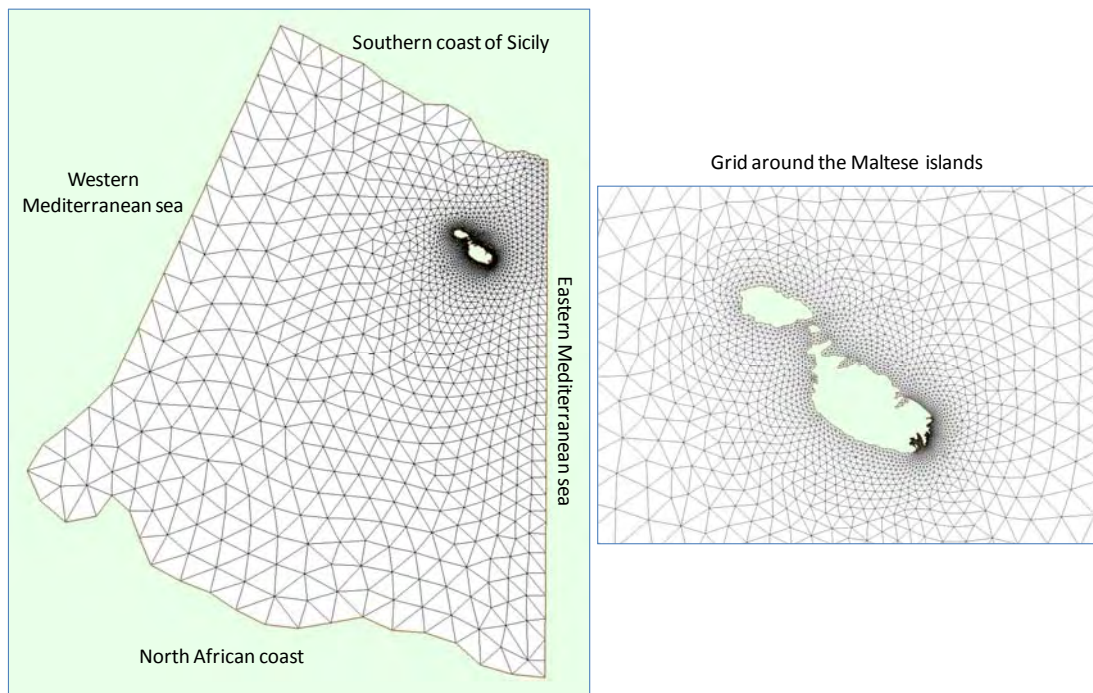
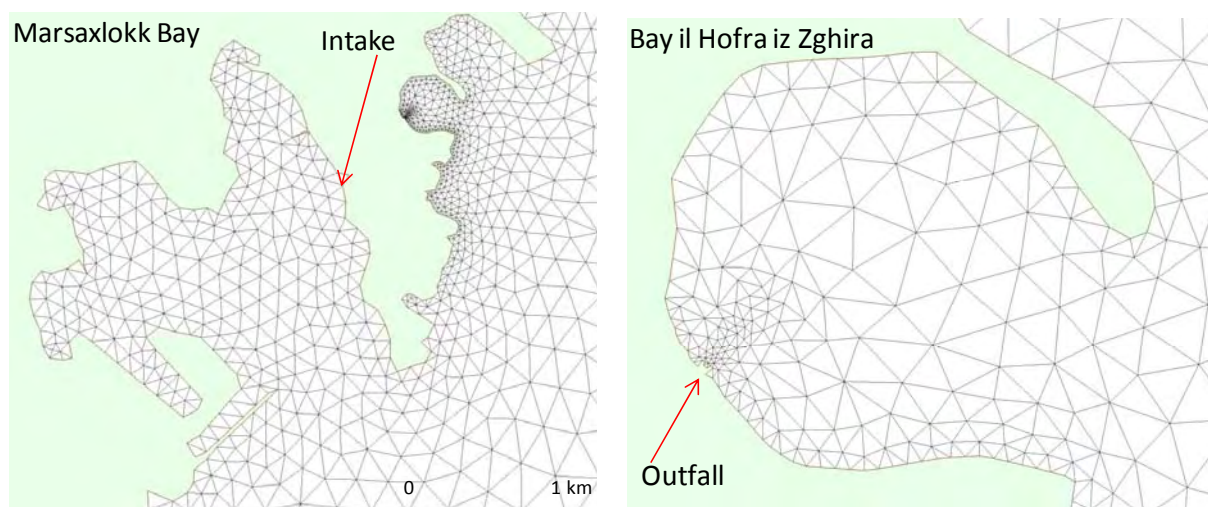


**Figure 5 Model Grid – Detail of DPS Intake & Outfall**



### 3.2 Water Depth Data

Figure 6 and Figure 7 show the combined water depth over the whole model area and at the DPS intake and outfall. Water depths have been taken from Euronav Seapro software and Admiralty charts 2538 and 36. Information has also been obtained from the hydrographers at Transport Malta.

Depths are shown with respect to chart datum. Depths are generally digitised to the 10 m contour and interpolated to 1 m near the coast. Depths in the bays and harbours to the east and west of the Delimara power are as detailed as possible.

**Figure 6 Water Depths (m) to Chart datum: Model overview**

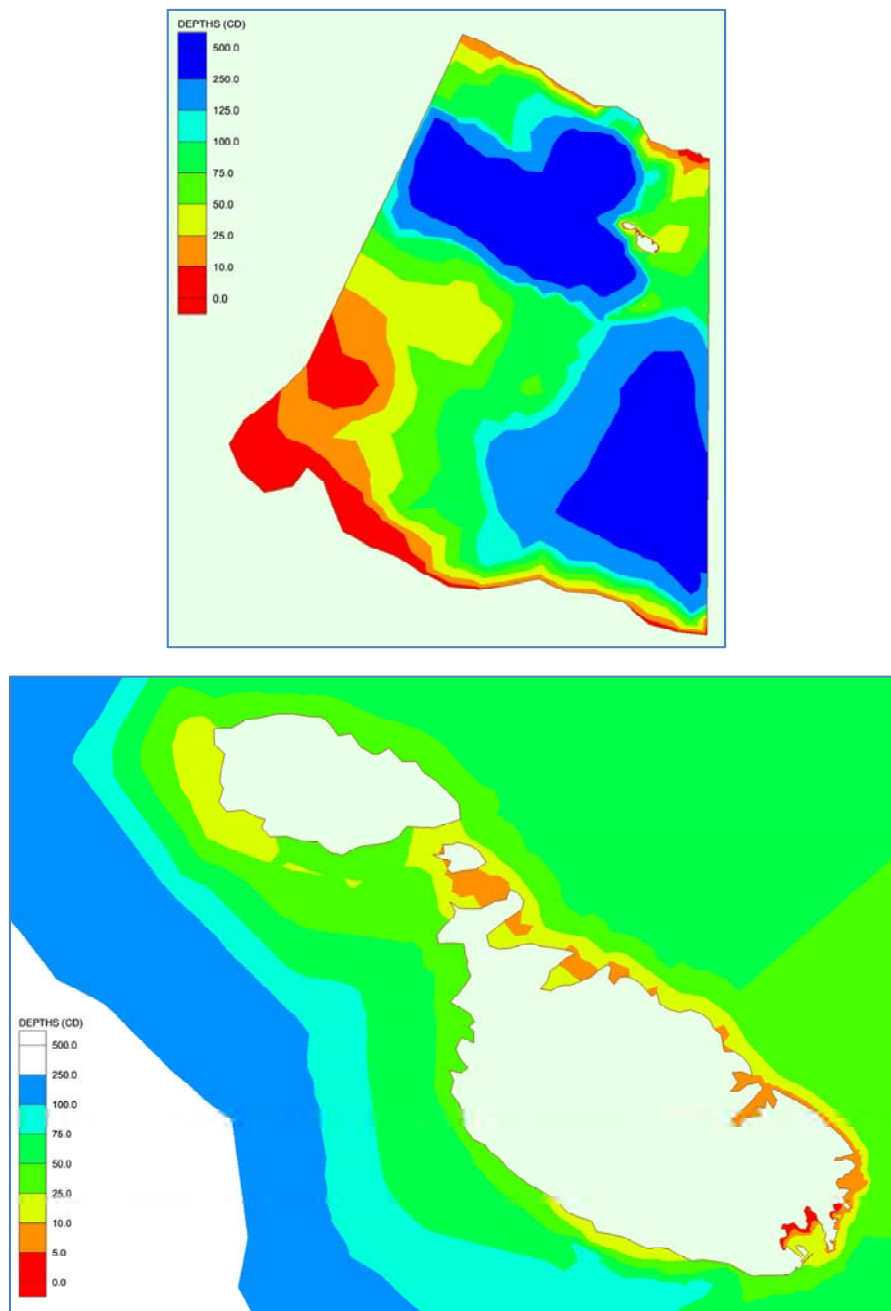
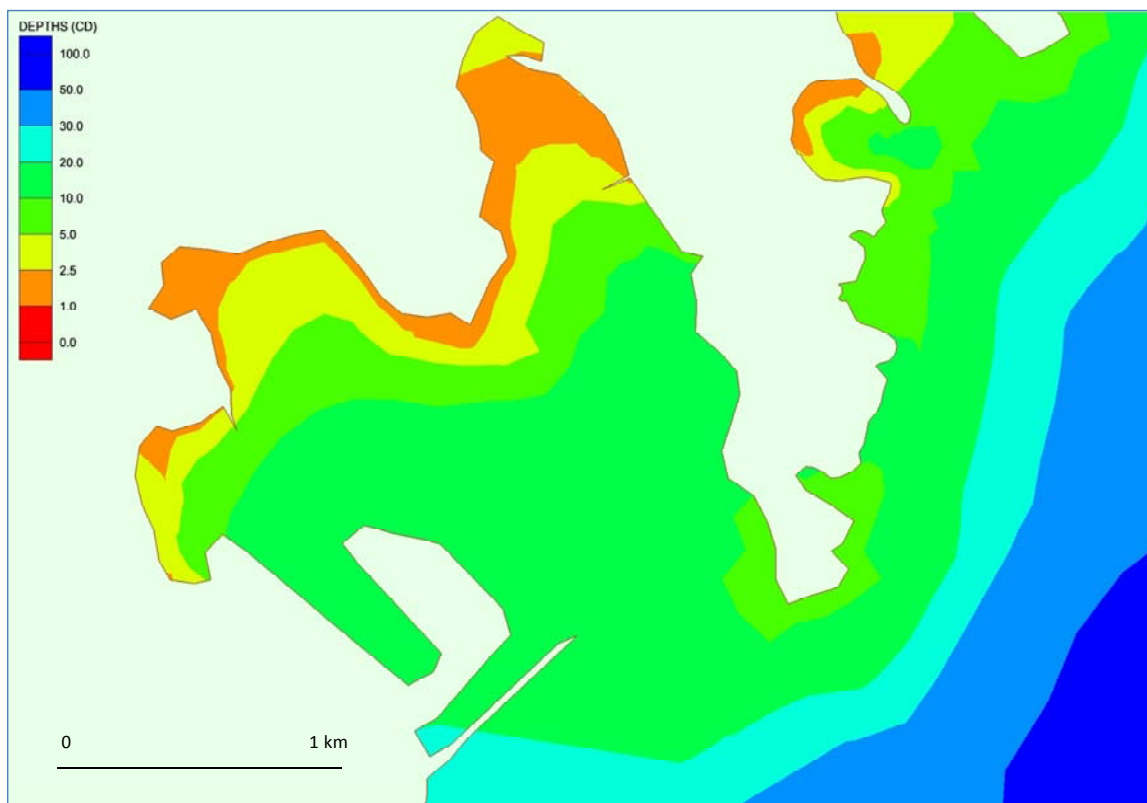


**Figure 7 Water depths (m) Chart datum: at DPS**



### 3.3 Water Movement

Modeling has accommodated complex water movement factors in the Mediterranean Sea. Information has also been obtained tidal flow from the hydrographers at Transport Malta for Freeport (Birzebbugia/Marsaxlokk bay) and Valletta Grand Harbour.

- Tidal flows are weak and reduce with distance east from the Straits of Gibraltar;
- Water circulation is complex; surface water moving overall from west to east;
- Circulation is driven by evaporation and is stronger in the summer than in winter;
- Wind driven currents are important and affect the surface water layers; and
- Currents can be driven by short-term seiches (oscillations in water level).

A detailed description of circulation patterns can be found at [http://www.1yachtua.com/mediterranean/Mediterranean\\_Sailing/mediterranean\\_currents.shtml](http://www.1yachtua.com/mediterranean/Mediterranean_Sailing/mediterranean_currents.shtml).

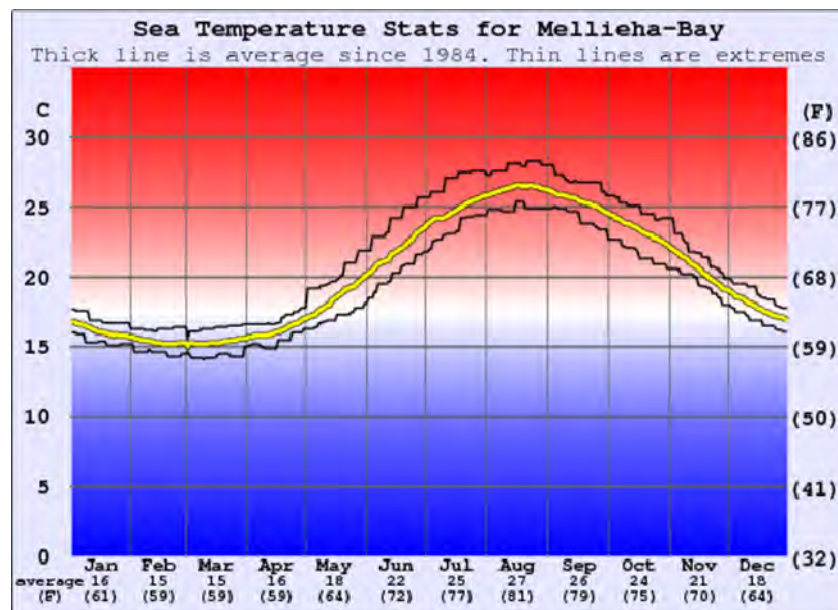
### 3.4 Temperature

Modeling uses the 15°C winter (February) and 27°C summer (August) temperature for the central Mediterranean Sea. Periodic summer heatwaves increase surface sea temperature to over ~29°C.

Figure 8 shows average and extremes of the annual temperature at Mellieha-Bay situated at the north-east of Malta (<http://www.surf-forecast.com/breaks/Mellieha-Bay/seatemp>).

The discharged cooling water has been taken to have a temperature 8°C higher than the background seawater.

**Figure 8 Measured Sea Water Temperatures at Mellieha-Bay, Malta.**



## 4.0 MODEL RESULTS

Results from the model predictions are presented in three sections:

- Tidal influences, waves and winds
- Tidal plus the Mediterranean circulation
- Tidal, circulation and seiche effects

Sections below present the predicted temperatures for the existing and increased flow rate, and for winter and summer conditions.

### 4.1 Tidal Influences Waves & Winds

Tides are taken as the basic flow in the area, though it is known that the tidal currents are weak and generally dominated by the other processes listed above.

The driving force for the tides in the model area are the changing tidal heights at the south-west (La Goulette, Tunisia), north-west (Marsala, west Sicily), north-east (Catania, east Sicily) and south-east (Misratah, Libya) corners of the model.

Table 1 shows tidal elevations at each of these ports calculated from the tidal Harmonics given in the Admiralty Tide Tables<sup>2</sup>. The harmonic constants for Valletta, on Malta, are also given as these can be used as one form of model validation. Figure 9 shows example plots of a neap to spring to neap cycle of tides (in centimetres) for each port.

**Table 1 Harmonic Constants for Water Elevation**

Port	Country	Port number	Z <sub>0</sub>	M2-g	M2-H	S2-g	S2-H	K1-g	K1-H	O1-g	O1-H
La Goulette	Tunisia	1828	0.3	278	0.08	304	0.03	211	0.03	130	0.01
Marsala	Sicily	1868	0.15	265	0.07	277	0.02	163	0.04	123	0.02
Catania	Sicily	1871	0.12	90	0.06	97	0.03	61	0.01	57	0.01
Misratah	Libya	1997	0.37	111	0.07	132	0.04	96	0.02	141	0
Valletta	Malta	1880	0.63	83	0.12	92	0.07	36	0.02	81	0.01

Port locations are effectively the at the "corners" of the mathematical model plus at Valletta, Malta  
Z<sub>0</sub> – mean tide level (m) relative to the local datum, M2 – lunar semi-diurnal tide, S2 – solar semi-diurnal tide, K1 – lunar diurnal tide, O1 – lunar diurnal tide, H – tidal amplitude (m), g – tidal phase (degrees)

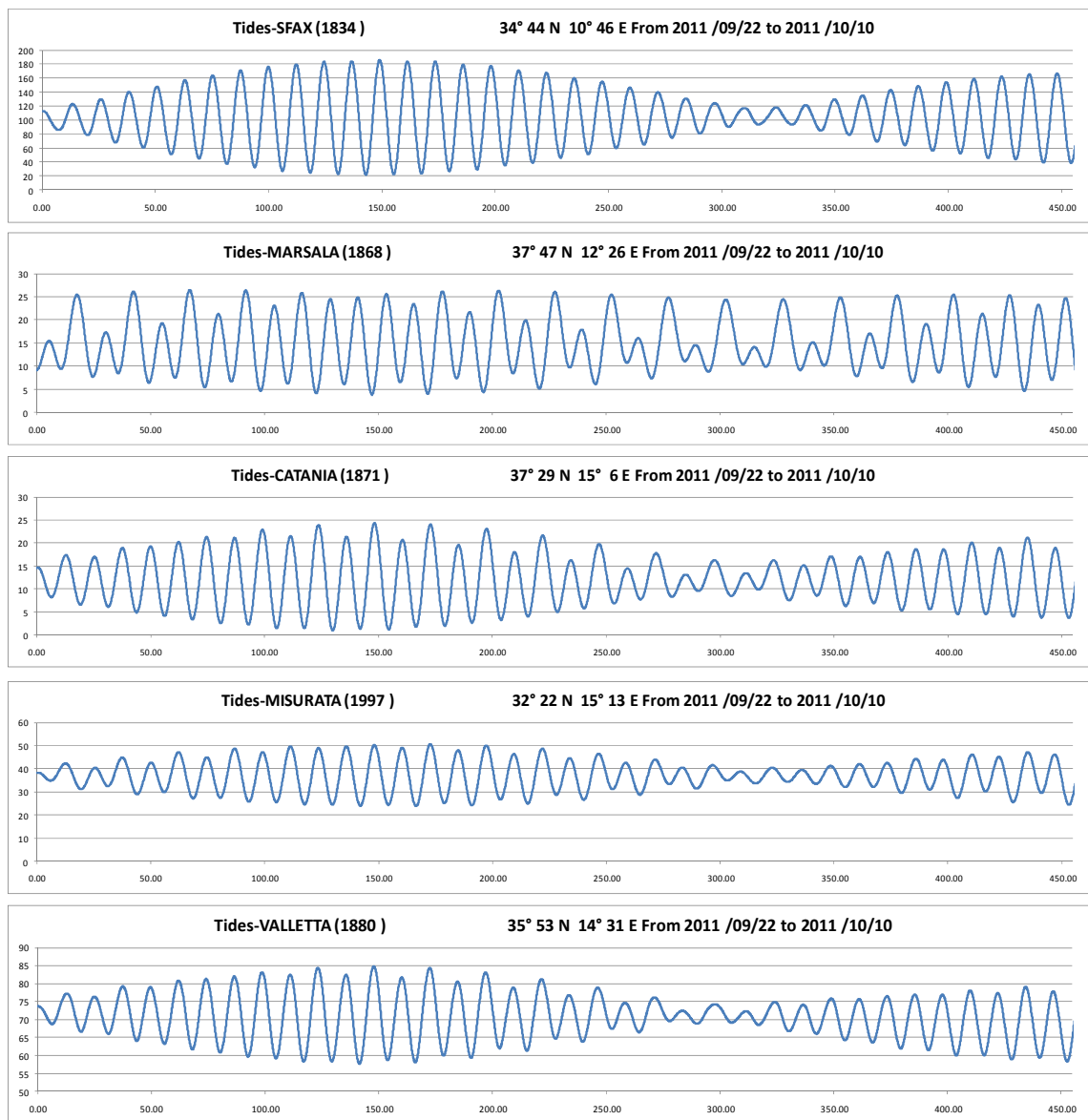
Tidal harmonics for La Goulette, Marsala, Catania and Misurata are entered into the FVCOM model, which uses the data to generate tidal heights at each grid node along the western boundary and along the eastern boundary of the model area (Figure 4).

There are no measurements of tidal flows in the coastal waters adjacent to Marsaxlokk or il Hofra iz Zghira that can be used to check the model predictions. Predicted tidal currents are shown in Figure 10 & Figure 11. Flows inside Marsaxlokk inlet (Figure 10) are of the order of 1 cm/s and in il Hofra iz Zghira (Figure 11) less than 1 cm/s. Flows along the coast are 3 to 10 cm/s and reverse with the tide.

<sup>2</sup> UK Hydrographic office (2011). Admiralty Tide Tables Volume 2 2012 Europe (excluding United Kingdom and Ireland), Mediterranean Sea and Atlantic Ocean.



**Figure 9 Tidal Elevations (cm) for 22/9/2011 to 10/10/2011 (hours)**



With the existing DPS discharge present the flows in il Hofra iz Zghira are dominated by the outfall; at the outfall currents reach 0.88 m/s for the existing discharge. The flow pattern in the bay changes (Figure 12). With the outfall, water flows flush around the bay and out into the coastal zone at all times; current speeds are between 1 and 25 cm/s within the bay and approximately 10 cm/s across the mouth of il Hofra iz Zghira into the coastal waters. The outflow from il Hofra iz Zghira modifies the flow pattern in the coastal zone for distance of approximately 700 m offshore (compare Figure 11 and Figure 12) and for almost 2.5 km along the coast.

For the proposed increase in discharge flow the currents near the outfall increase to 1.28 m/s, and the flow across the mouth of il Hofra iz Zghira into the coastal waters is approximately 15 cm/s.

**Figure 10 Tidal Flow Marsaxlokk inlet: No Discharge  
Flood Tide (top) & Ebb Tide (bottom)**

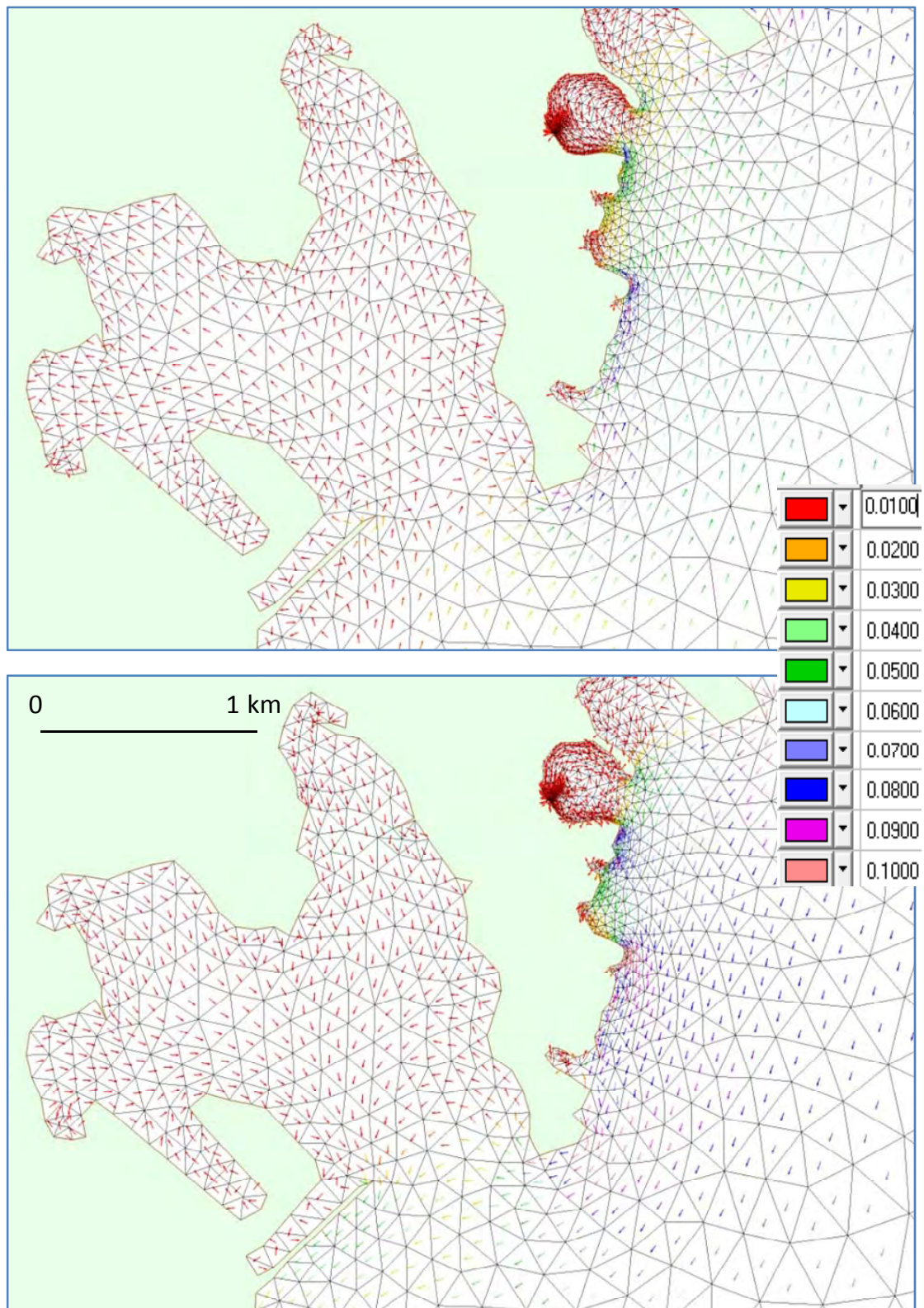




**Figure 11 Tidal Flows in il Hofra iz Zghira: No Discharge  
Flood Tide (top) & Ebb Tide (bottom)**

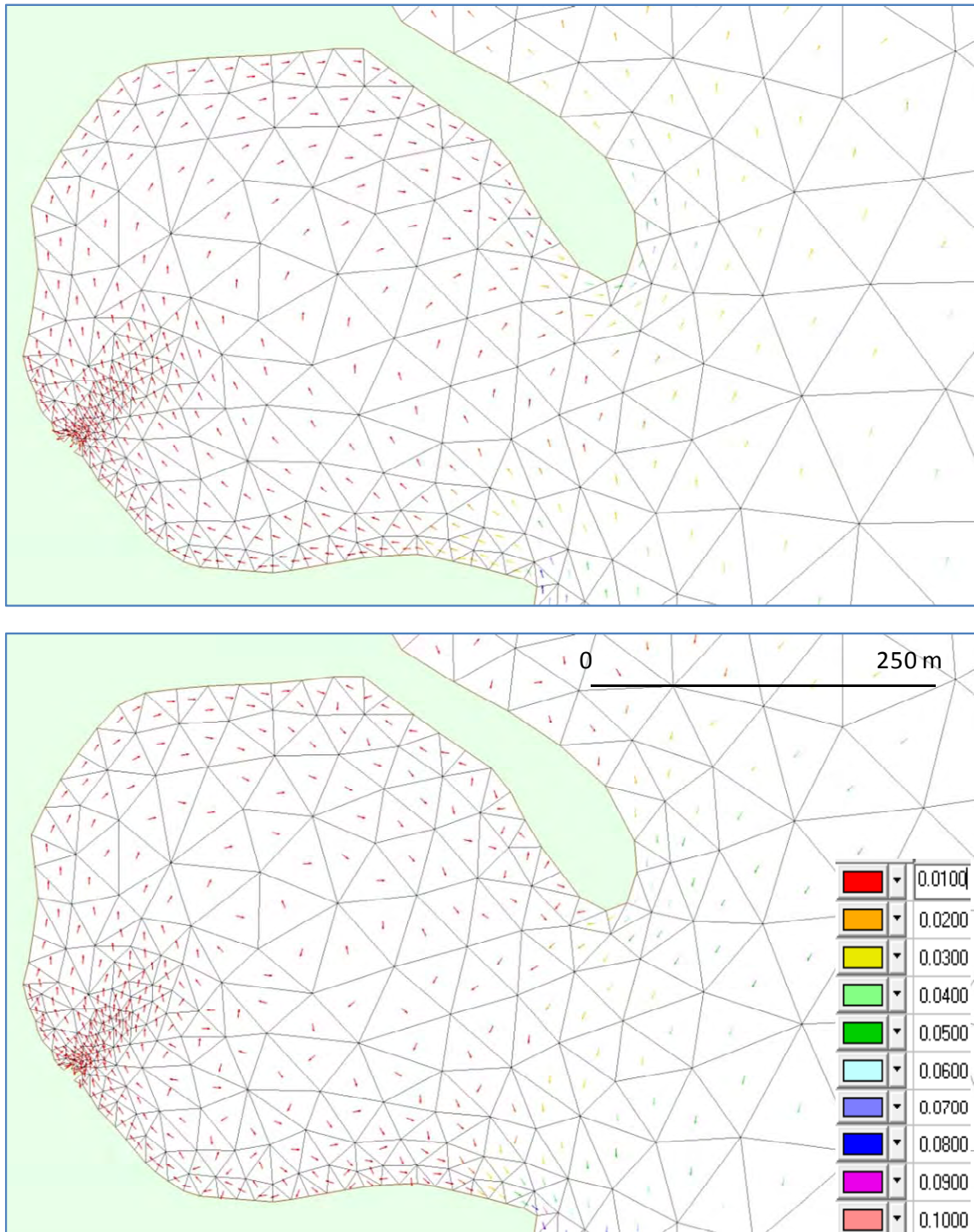
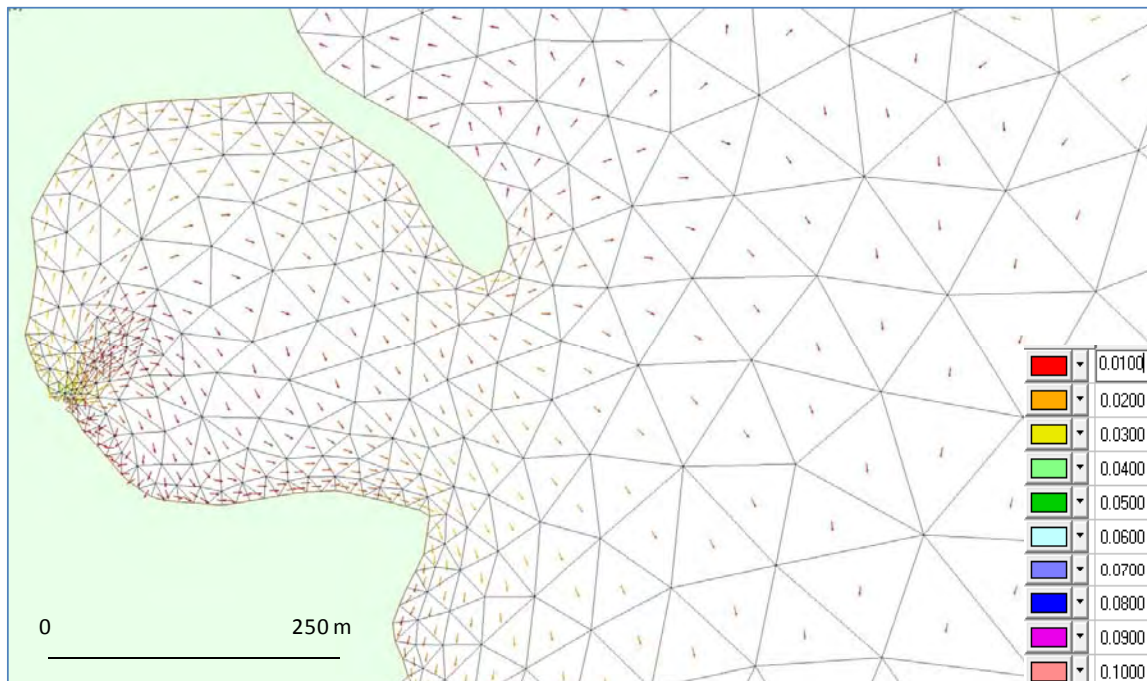


**Figure 12 Flows in il Hofra iz Zghira: Existing DPS Discharge**



#### **4.1.1 Temperature for the Existing Discharge**

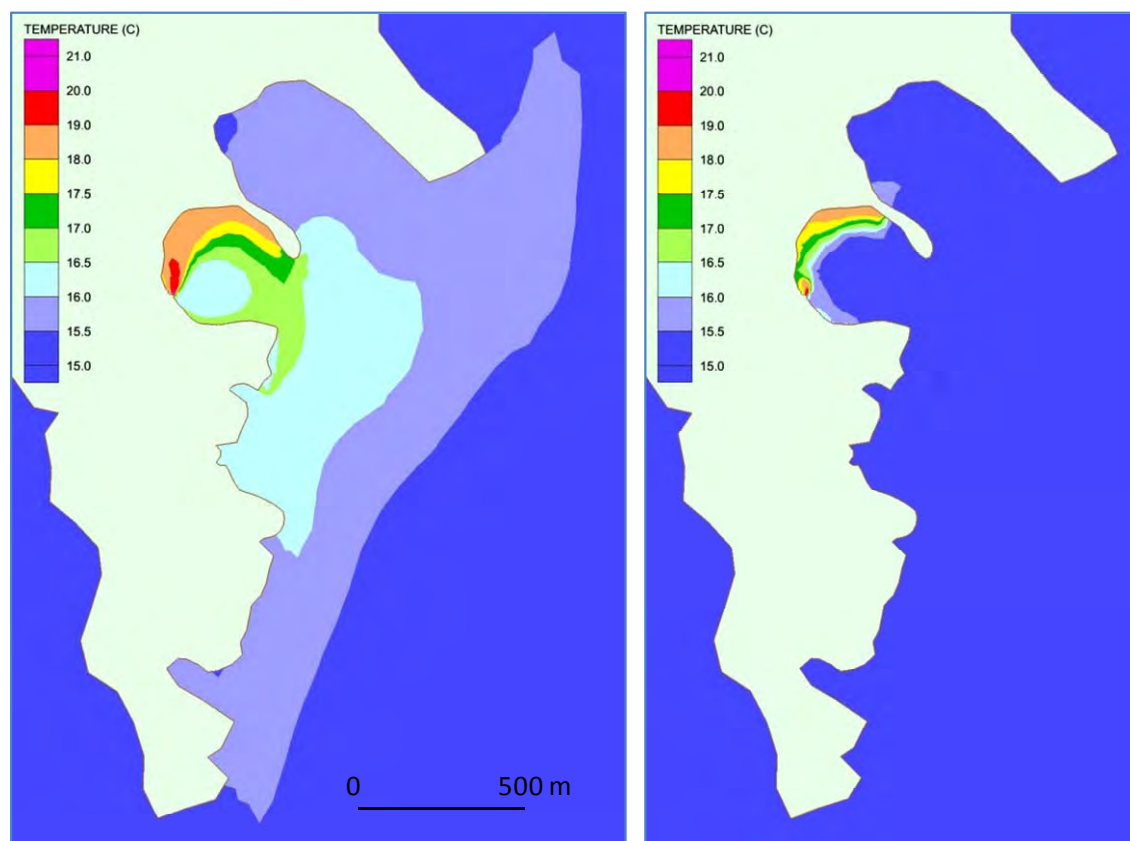
Figure 13 shows the predicted temperature plume at the water surface and at the seabed from the existing DPS discharge for winter conditions.

The 15.5°C (+0.5°C) contour at the water surface extends approximately 1500 m south of the bay and 1000 m north and the +1.0°C contour extends 750 m to the south. Water of 16.5°C protrudes from the bay with a tongue extending approximately 200 m to the south. Within il Hofra iz Zghira temperatures increase to +5°C (20°C) as the outfall is approached, however the area with temperatures  $\geq +5^\circ\text{C}$  is only 25 × 10 m.

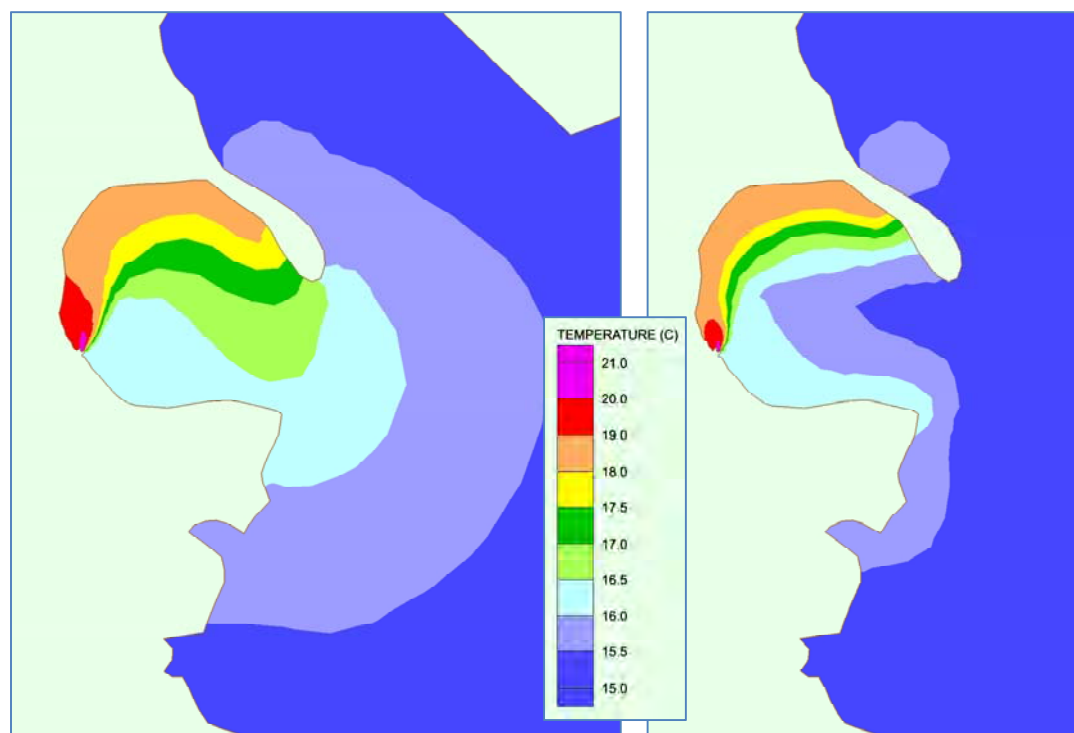
Figure 13 (right plot) shows increased sea bed temperatures only occur in the shallow areas around the western and northern edges of the bay. With low tidal currents there is little turbulence in il Hofra iz Zghira and the vertical mixing of the heated water is minimal. Predictions show no increase in temperature at the north and south points marking the mouth of the bay and no temperature increase on the seabed outside of il Hofra iz Zghira.

Figure 14 shows sea surface and sea bed temperatures when there is significant wave action in il Hofra iz Zghira and the adjacent coastal waters. Wave action can increase the vertical mixing and spread the heated water plume down into the water column resulting in a wider area of the seabed being influenced by the warmer water. Wave mixing causes a significant reduction in the areas of sea surface with both +0.5°C and +1°C temperature increases above background (compare Figure 13 & Figure 14). Sea bed temperatures outside of the bay are affected and can be up to 0.5°C above background, but only within 75 m of the coast for 300 m to the south of the bay. On the southern point of the mouth of il Hofra iz Zghira a seabed temperature of 16°C (+1°C) is predicted. Within the bay the highest temperatures on the bed occur around the western and northern edges.

**Figure 13 DPS Existing Discharge Winter Conditions:  
Surface temperatures (left) & Seabed temperatures (right)**



**Figure 14 DPS Existing Discharge Winter Conditions with Significant Wave Action:  
Surface temperatures (left) & Seabed temperatures (right)**



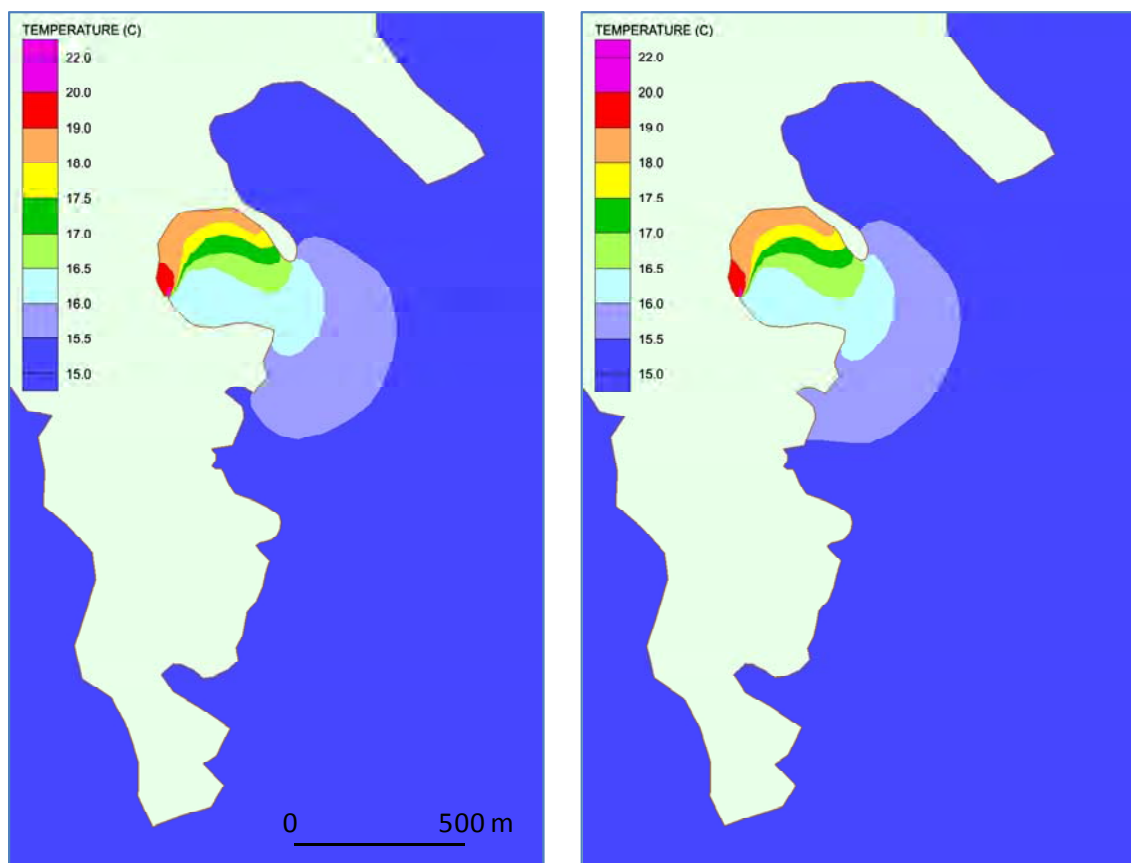


Wind affects the movement and spread of a cooling water plume. In Malta the two main wind directions are north-west (the Majjistral) and north-east (the Grigal). These two winds are likely to have the greatest effects on the DPS plume. The Majjistral would be expected to spread the plume more rapidly out of il Hofra iz Zghira and promote dispersion whereas the Grigal would hold the plume in the bay and reduce the rate of dilution and cooling. Mean wind speeds are 4.6 m/s for September and 7.6 m/s for December. Other wind directions are less likely to affect the plume spread to any significant degree.

For light to medium winds (0 – 5 m/s) the predicted effects on the warm water plume are negligible. With stronger wind speeds (e.g. 10 m/s) the vertical mixing in the water column is increased and the simulated warm plumes are similar to Figure 14 for wave action.

Figure 15 shows the predicted temperature plume in winter for north-west and north-east wind directions (10 m/s). Plots show there is little effect on the plume temperature contours, particularly within il Hofra iz Zghira Bay, which indicates that the increased vertical mixing dominates over the effects of the wind altering the water velocities at the surface.

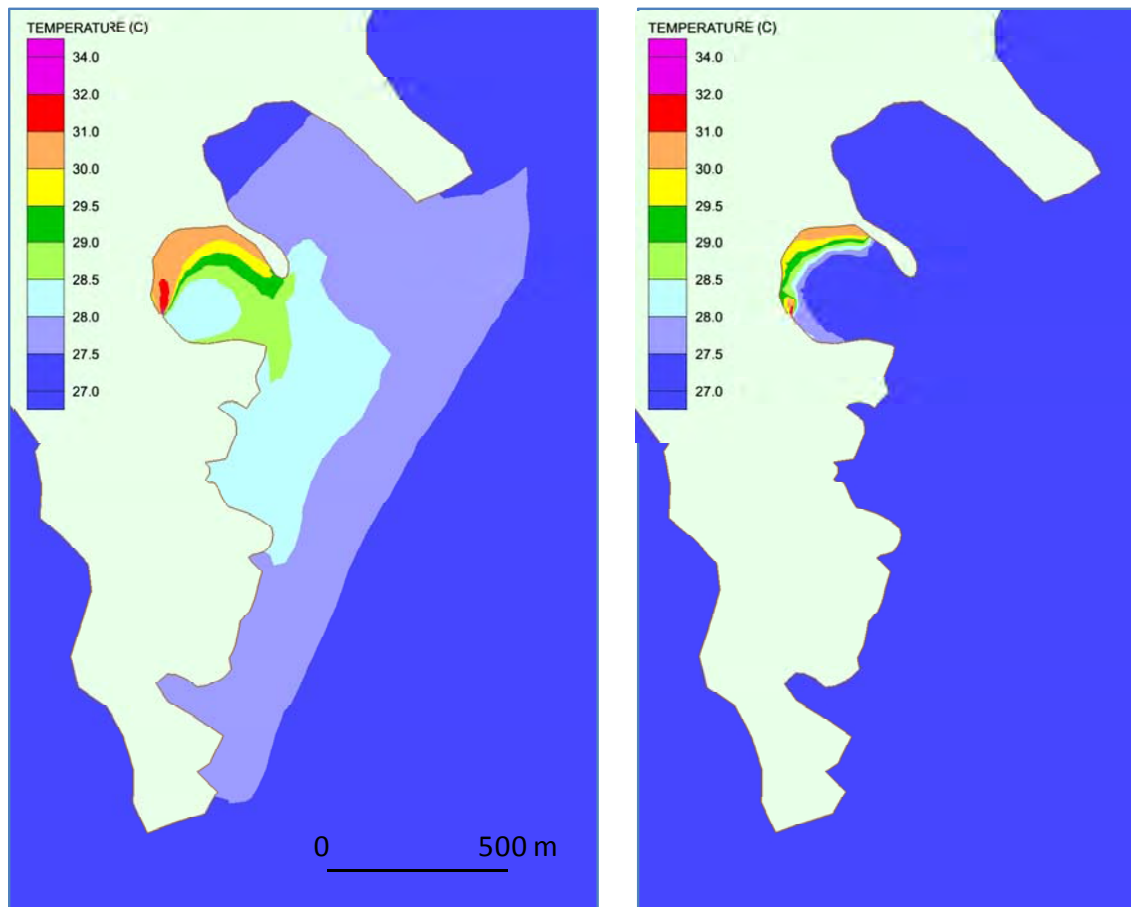
**Figure 15 DPS Existing Discharge Winter Conditions:  
North-West wind 10 m/s (left), North-East 10 m/s wind (right)**



Predicted sea surface and seabed temperatures for summer are shown in Figure 16. The temperatures are approximately 12°C higher than in winter, but the patterns of temperature increase above background levels are similar to those predicted for winter conditions.

The effects of waves and winds in summer follow the same patterns as in winter and are therefore not shown.

**Figure 16 DPS Existing Discharge Summer Conditions:  
Surface temperatures (left) & Seabed temperatures (right)**



#### **4.1.2 Temperature for the Increased Discharge**

Figure 17 shows the predicted temperature plume at the water surface and at the seabed from the increased power station discharge for winter conditions.

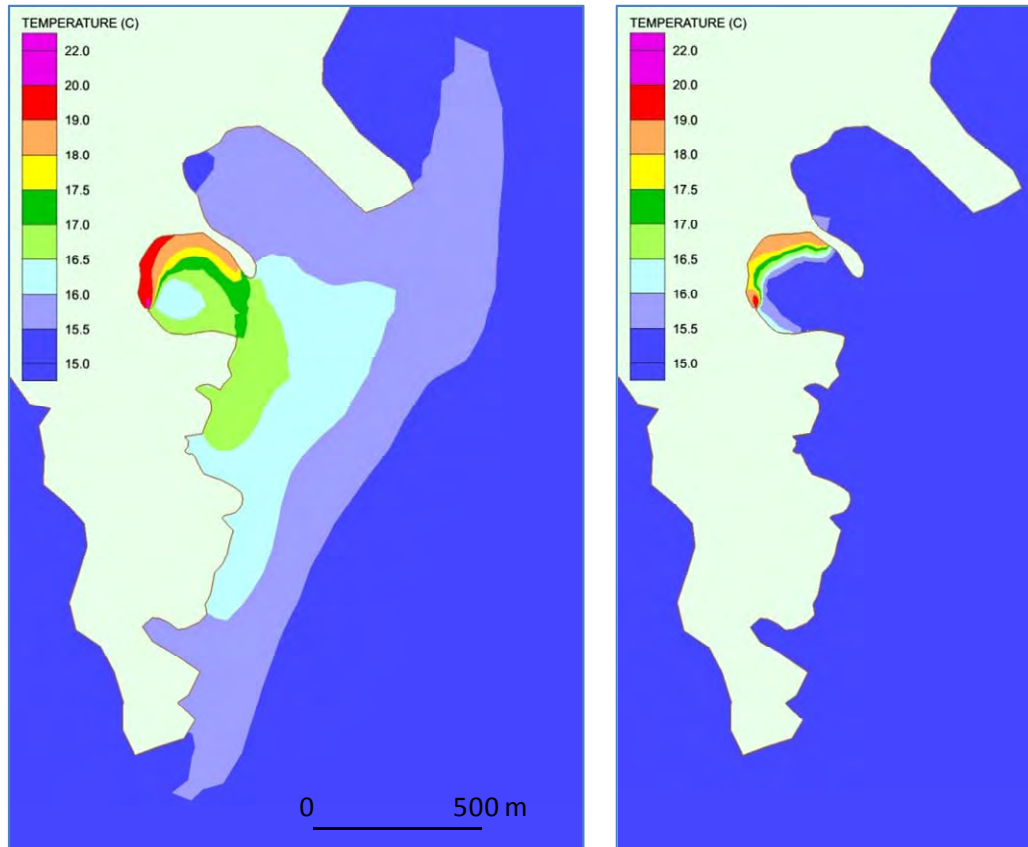
The 15.5°C (+0.5°C) contour at the water surface extends approximately 1750 m south of the bay and 1200 m north and the +1.0°C contour extends 1100 m to the south. Water of 16.5°C protrudes from the bay with a tongue extending approximately 450 m to the south. Within il Hofra iz Zghira temperatures increase to +5°C (20°C) as the outfall is approached, and the area with temperatures  $\geq +5^\circ\text{C}$  is predicted to be approximately  $48 \times 13$  m.

Figure 17 (right plot) shows increased sea bed temperatures only occur in the shallow areas around the western and northern edges of the bay. Due to the low tidal currents there is little turbulence in il Hofra iz Zghira and the vertical mixing of the heated water is minimal. Predictions show no increase in temperature at the north and south points marking the mouth of the bay and no temperature increase on the seabed outside of il Hofra iz Zghira.

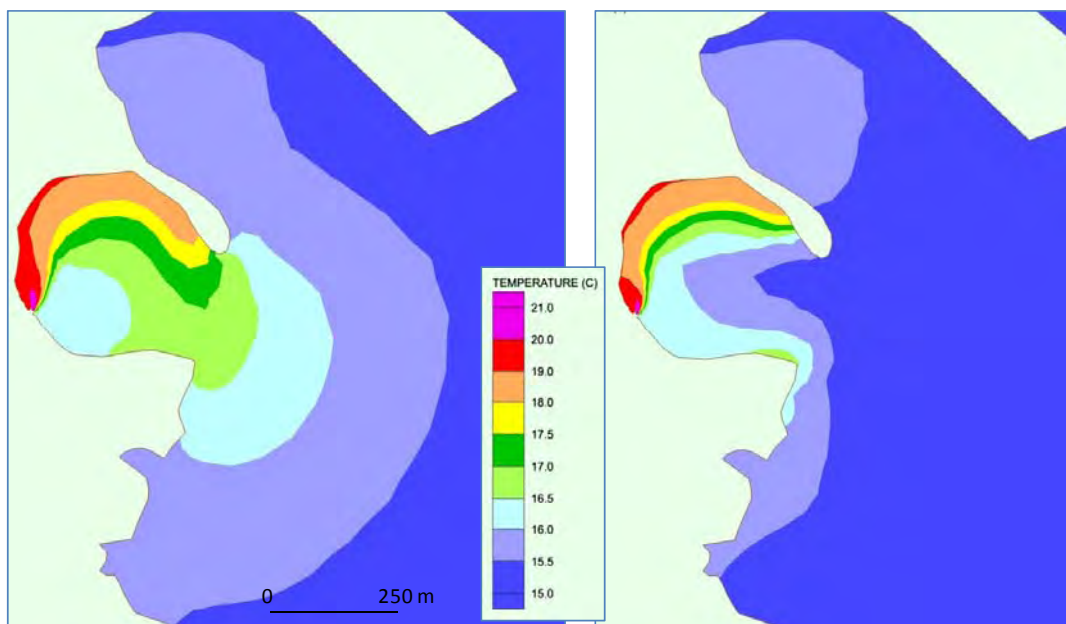
Figure 18 shows sea surface and sea bed temperatures when there is significant wave action in il Hofra iz Zghira and the adjacent coastal waters. Wave mixing causes a significant reduction in the area of sea surface with both +0.5°C (15.5°C) and +1°C (16°C) temperature increases above background (compare Figure 17 & Figure 18). Sea bed temperatures outside of the bay are now affected and can be up to 0.5°C above background, but only within 120 m of the coast for 480 m to the south of the bay, and within il Hofra i-Kbira which is immediately to the north of il Hofra iz Zghira. A tongue of water of

16°C reaches out of the southern end of the bay and hugs the coast to the south for 135 m. On the southern point of the mouth of il Hofra iz Zghira a seabed temperature just reaching 16.5°C (+1.5°C) is estimated. Within the bay the highest temperatures on the bed occur around the western and northern edges.

**Figure 17 DPS Increased Discharge Winter Conditions:  
Surface temperatures (left) & Seabed temperatures (right)**



**Figure 18 DPS Increased Discharge Winter Conditions & significant wave action:  
Surface temperatures (left) & Seabed temperatures (right)**



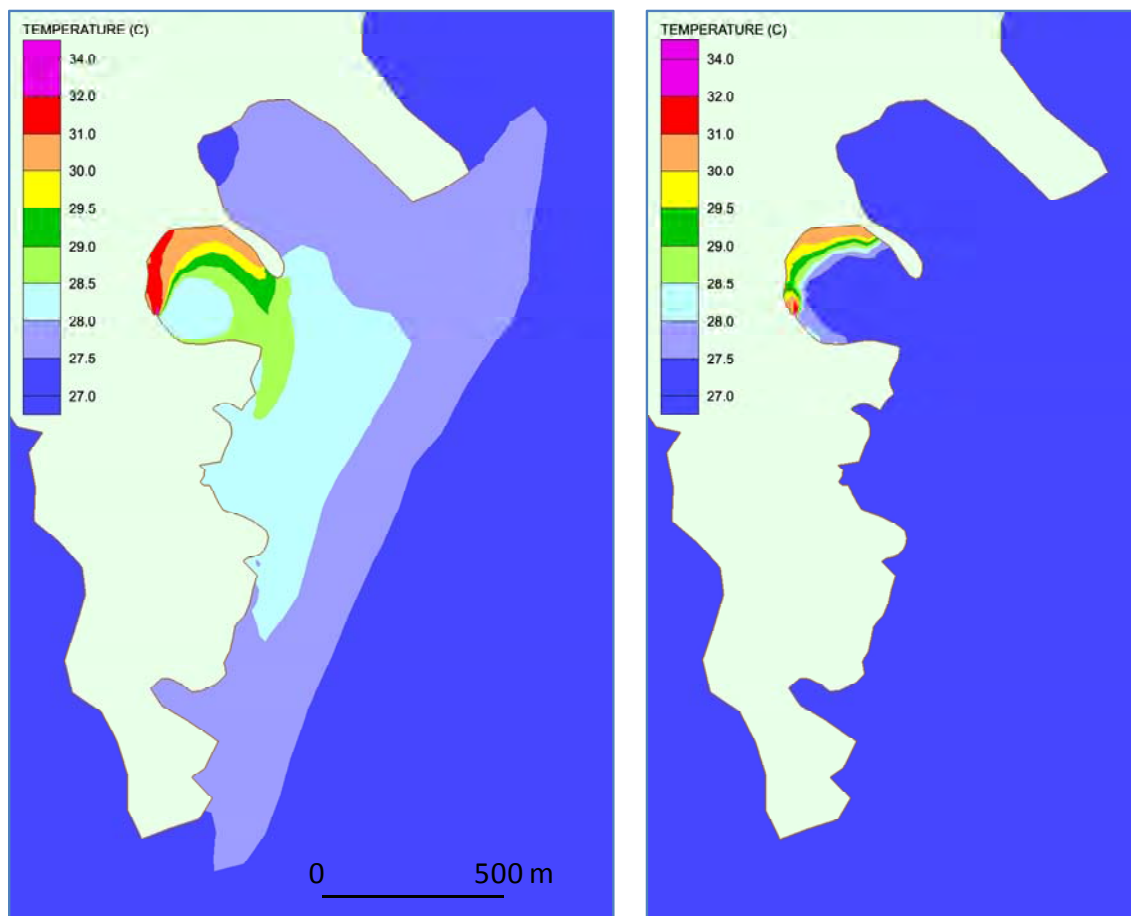


Wind effects on increased discharge plume are negligible for light winds (0 – 5 m/s) and dominated by increased vertical mixing for strong winds (similar to Figure 15 for the existing discharge rate).

Figure 19 shows sea surface and seabed temperatures for summer. Temperatures are approximately 12°C higher than in winter, but the pattern of temperature increase above background levels is similar to that predicted for winter conditions.

The effects of waves and winds in summer follow the same patterns as in winter and are therefore not shown in this report.

**Figure 19 DPS Increased Discharge Summer Conditions:  
Surface temperatures (left) & Seabed temperatures (right)**



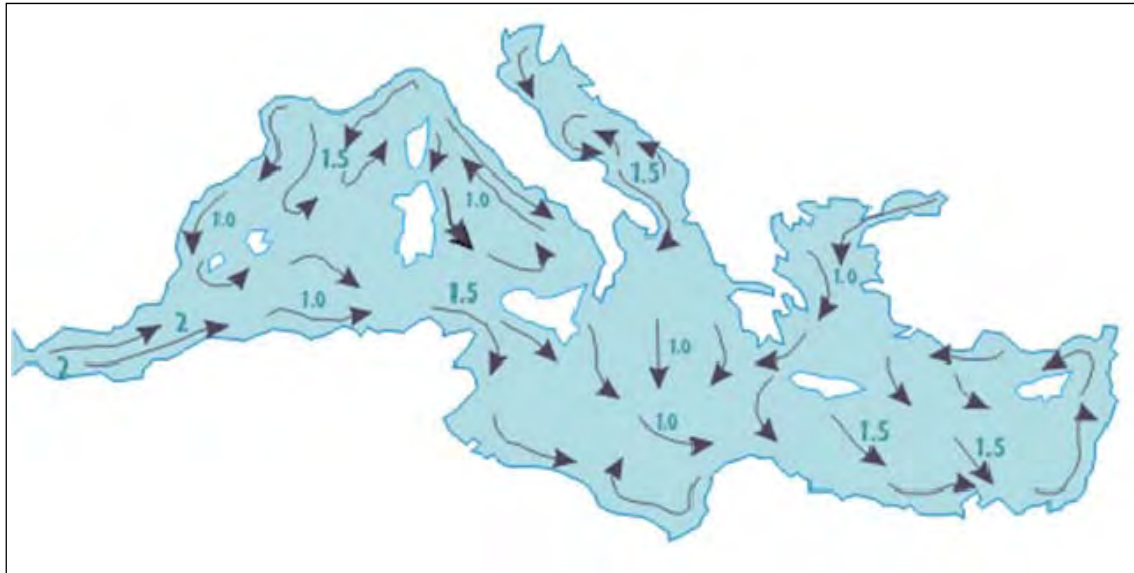
## 4.2 Tidal plus Mediterranean Sea Circulation

Figure 20 shows the general circulation pattern for the Mediterranean in June. The Sea has a general west to east water circulation driven by water evaporation from the sea surface causing the sea level to be lower in the east than in the west<sup>3</sup>. Current flows towards east-south-east in the region to the south of Sicily. The detail of the plot is not sufficient to include Malta and the magnitude of the current is not quantified.

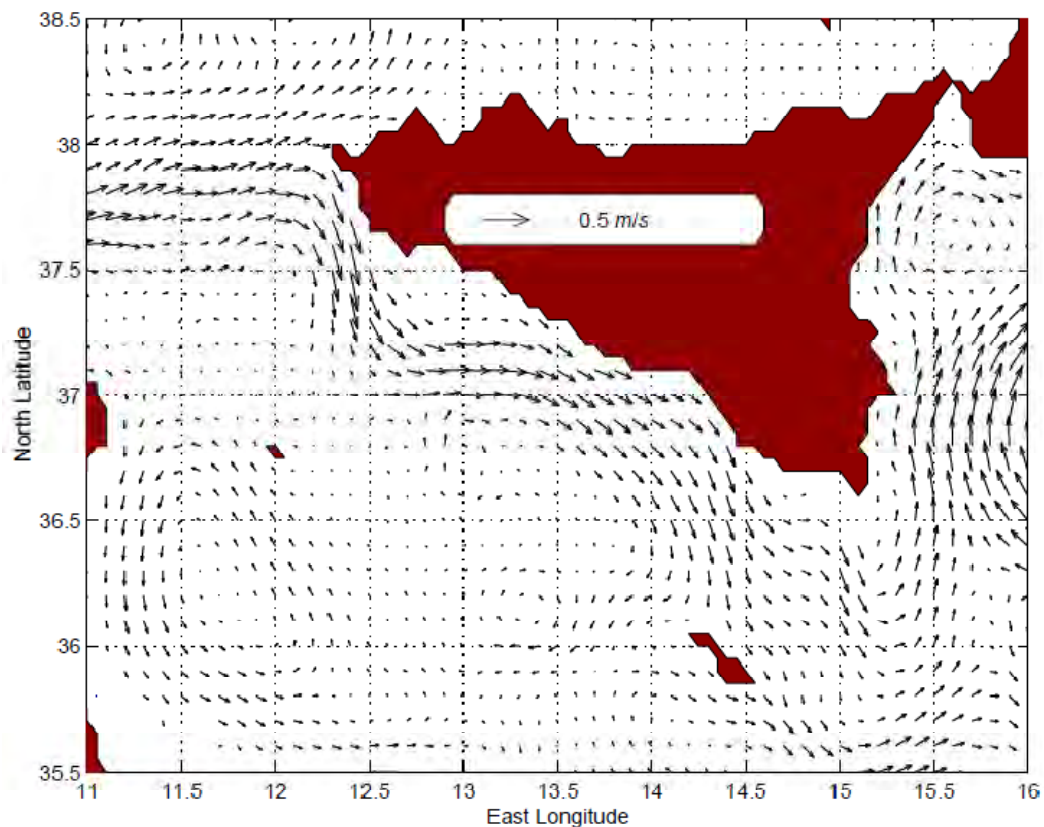
<sup>3</sup> [http://www.lyachtua.com/medit-marinas/Mediterranean\\_Sailing/mediterranean\\_currents.shtml](http://www.lyachtua.com/medit-marinas/Mediterranean_Sailing/mediterranean_currents.shtml)

Figure 21 (Sorgente *et al.*<sup>4</sup>) gives more detail in the central Mediterranean region. South-east flows of approximately 0.25 m/s flow down from the Sicily coast towards Malta and these flows weaken to between 0.15 and 0.2 m/s towards the eastern end of Malta.

**Figure 20 Mediterranean Sea General Water Circulation for June.**



**Figure 21 General Circulation Surface Flows for September by Sorgente et al. (2003)**



<sup>4</sup> Sorgente R, Drago A F, Ribotti A, 2003. Seasonal variability in the central Mediterranean Sea circulation. *Annales Geophysicae* 21: 299–322.

Boundary conditions for the FVCOM model have been modified by raising the tidal heights along the western boundary by 5 cm to produce an easterly flowing current. This modification only attempts to reproduce the flows between the southern coast of Sicily and Malta, not the gyres seen to the west and south of Malta. This is considered to be appropriate for the study of the DPS discharge, which only affects a very local area. Figure 22 shows the flows predicted by the FVCOM model, which are much more detailed than Sorgente *et al.*'s results but show the same directions and speed of water movement. The coastal flows are very similar to Sorgente *et al.*'s values, being approximately 20 cm/s. This is significantly greater than the 3-10 cm/s for the tide only simulations (Figure 10).

**Figure 22 Tidal plus Circulation Flows in the Surface Waters near DPS**

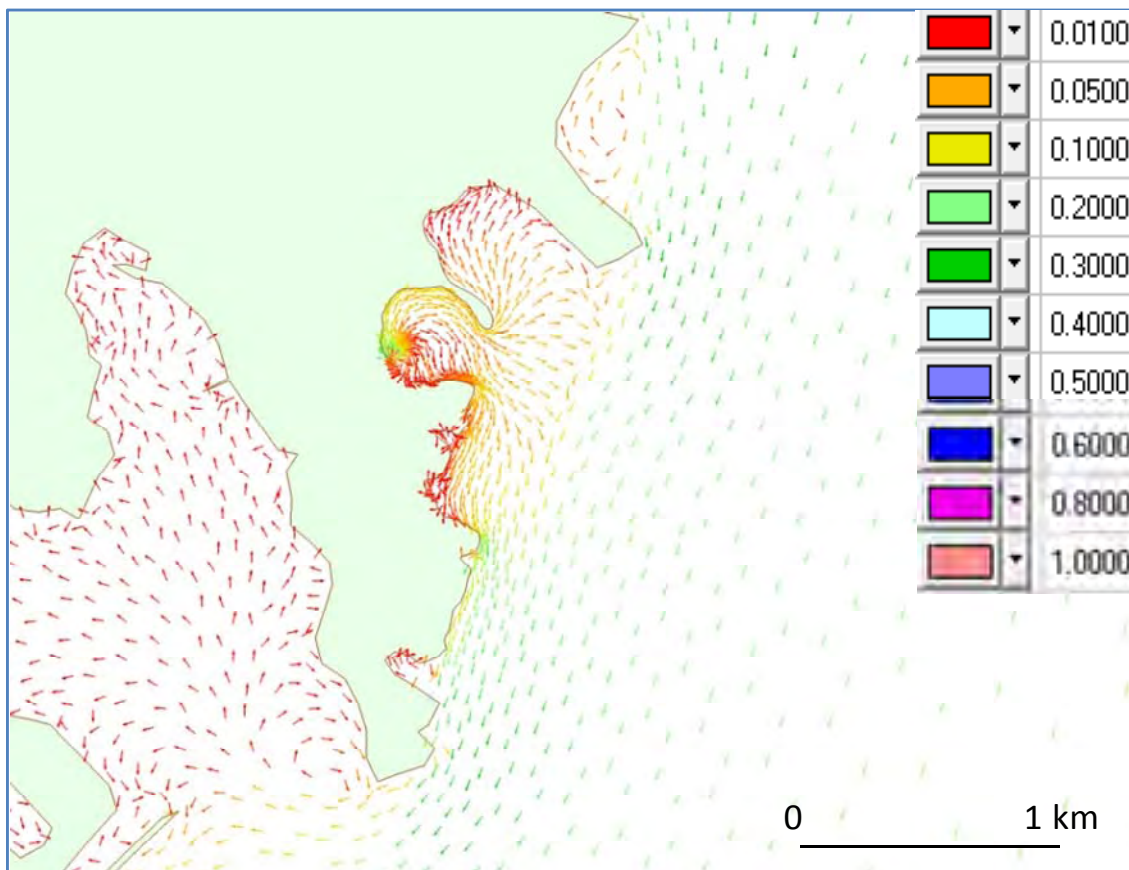
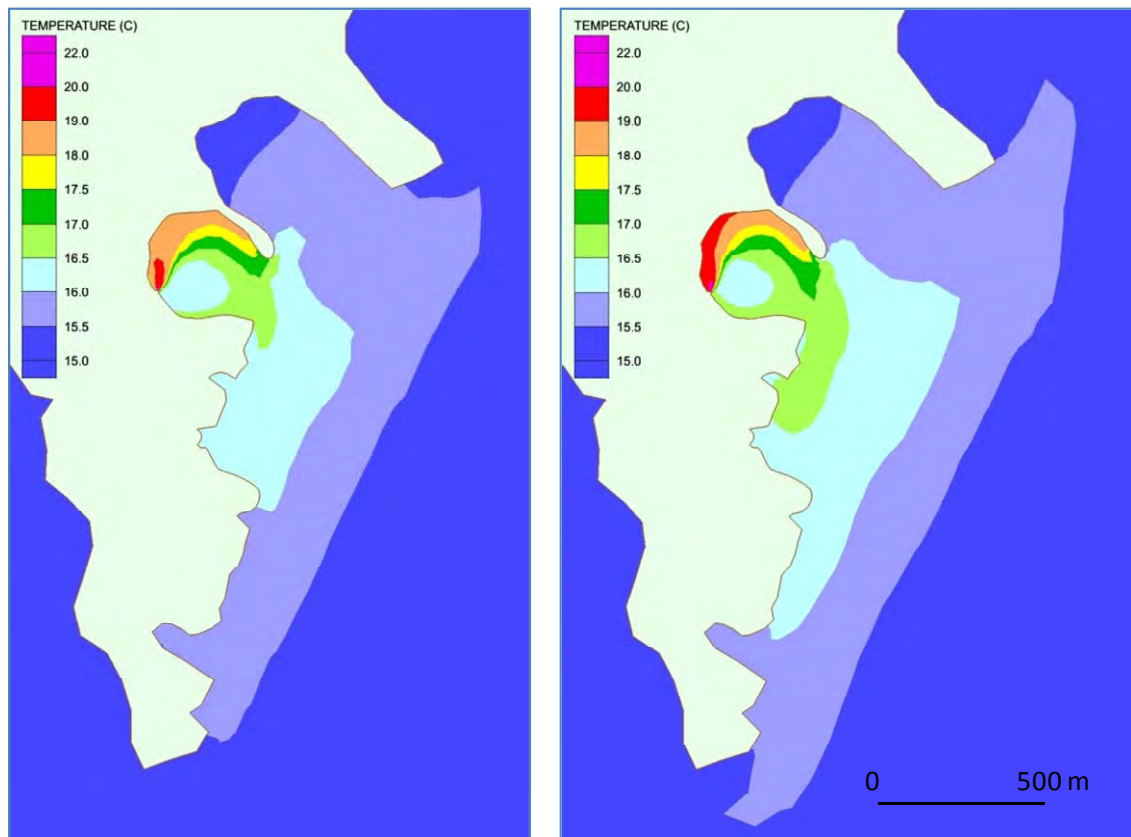


Figure 23 shows estimated winter temperatures for the existing discharge rate and the increased discharge rate with the additional effect of general circulation. Compared to the winter plots (Figure 13 & Figure 17) there is little difference in surface water temperatures for the two cases. This indicates that the movement and mixing of the plume is driven mainly by the energy of the discharge itself rather than the energy in the coastal flow.

**Figure 23 DPS Winter Conditions temperature for tidal plus circulation flows:  
Existing Discharge (left), Increased Discharge (right)**



Predicted sea surface and seabed temperatures for summer are approximately 12°C higher than in winter, but the patterns of temperature increase above background levels are very similar to those predicted for winter conditions and for the tide only simulations. The effects of waves and winds in summer follow the same patterns as in the winter tide only simulations and are therefore not shown in this report.

#### 4.3 Tidal, Circulation and Seiche effects

Seiches are common in the coastal waters of Malta and other Mediterranean islands. A seiche is defined as (<http://encyclopedia2.thefreedictionary.com/Sieche>): “A standing-wave oscillation of an enclosed or semi-enclosed water body, continuing pendulum-fashion after cessation of the originating force, which is usually considered to be strong winds or barometric pressure changes.”

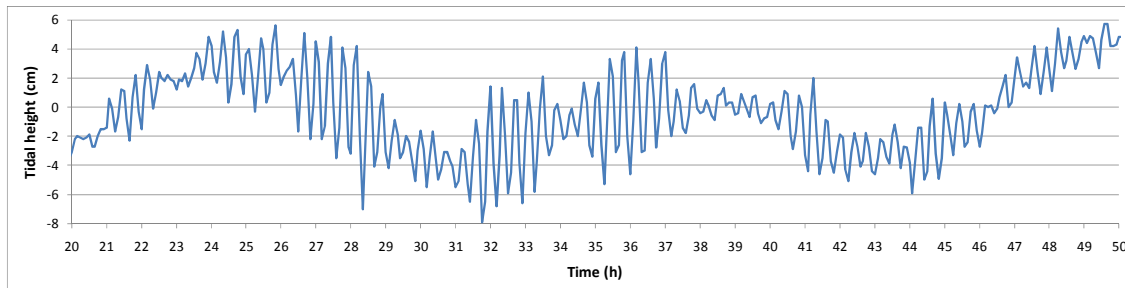
Seiches are reported along the north coast of Malta and are known as “the ‘milghuba’ waves” and have a frequency in the range 0.1 – 2 cycles per hour<sup>5</sup>. Tidal height measurements from the Grand Harbour in Valletta (Figure 24) show seiche effects superimposed on the tidal signal. Dr A Drago, Head of the Physical Oceanography Unit, University of Malta has studied the Maltese seiches in detail and the [http://www.gloss-sealevel.org/publications/documents/malta\\_2001.pdf](http://www.gloss-sealevel.org/publications/documents/malta_2001.pdf).

<sup>5</sup> Drago A, 2011. The Milghuba phenomenon in the Maltese Islands. Physical Oceanography Unit, University of Malta (pdf of “The Milghuba (Seiche) phenomenon in the Maltese Islands”) (<http://www.everythingselectric.com/forum/index.php?topic=65.0>)



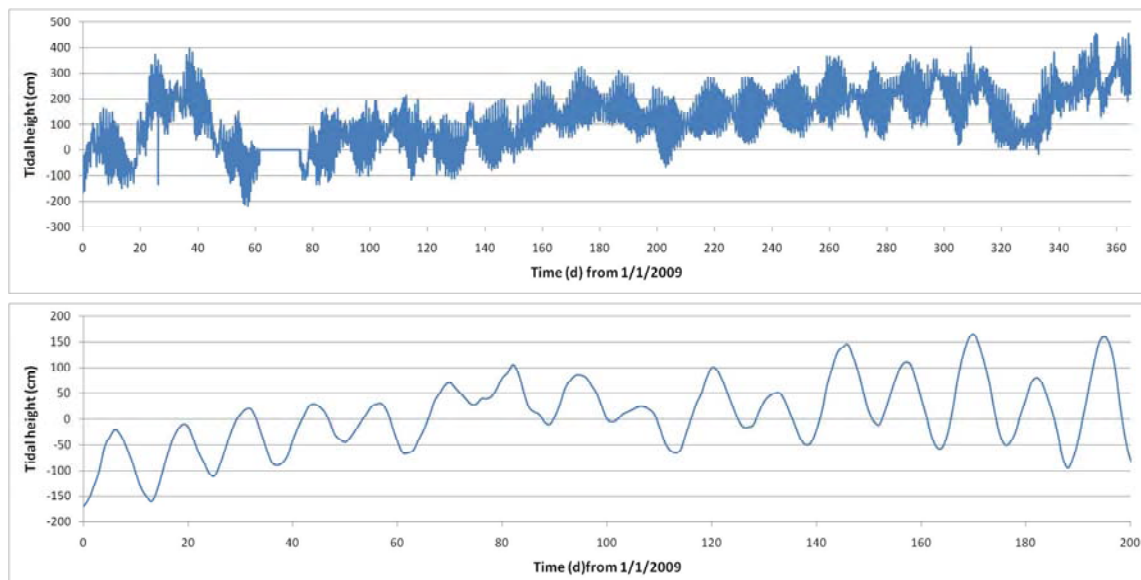
Web searches have not revealed any information on the presence or absence of seiches on the east end of Malta and in particular in Marsaxlokk inlet and il Hofra iz Zghira bay. Tidal height measurements in Marsaxlokk bay for the year 2009 do not show seiche activity and the tidal signal can be clearly seen (Figure 25). However since the measurements in this data set are hourly one cannot be sure there is no seiche activity.

**Figure 24 Tidal Heights, Grand Harbour, Valletta (23/24th June 2011)**



Digital Tide Gauge,

**Figure 25 Tidal heights, Marsaxlokk Bay: 2009 (top), detail (bottom)**



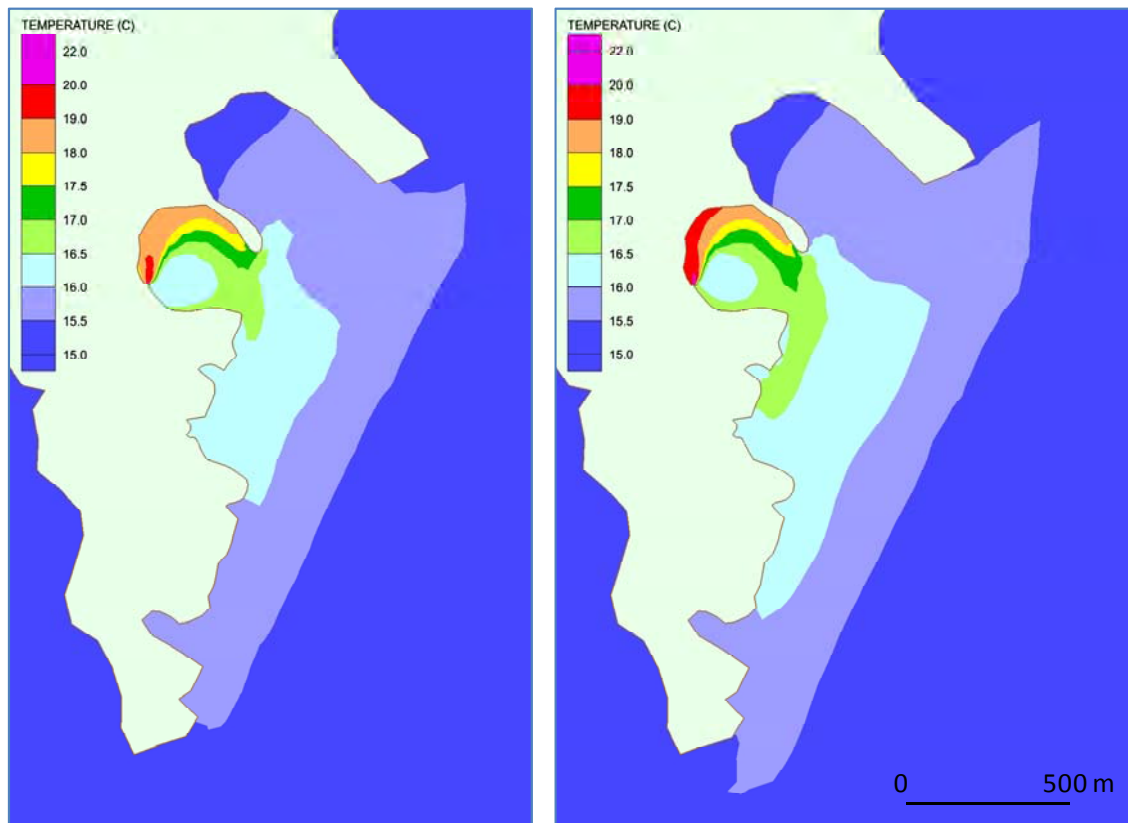
Mechanical tide gauge

The current model is not suitable to accurately simulate seiche activity which, in this area, is driven by fluctuations in atmospheric pressure<sup>5</sup>, however an approximate simulation is carried out by superimposing a 20 minute period seiche of amplitude 40 cm on the tidal boundary conditions of the model and allowing this to propagate through the model domain.

Figure 26 shows winter temperatures for the current discharge rate and the increased discharge rate with tidal, circulation and seiche flows. When compared with the tide only plots in Figure 13 and Figure 17 and the tide plus general circulation predictions in Figure 23 it can be seen that there is very little difference in the surface water temperatures for the different cases. This confirms that the movement and mixing of the warm water plume is driven mainly by the energy of the discharge itself rather than the energy in the coastal flow.

Once again the summer time patterns of increased temperature are very similar to the winter results and are therefore not shown.

**Figure 26 DPS Winter Conditions: Tidal, Circulation and Seiche flows:  
Existing Discharge (left), Increased Discharge (right)**



## 5.0 ENVIRONMENTAL IMPACT

### 5.1 Sensitive Receptors

The location of potentially sensitive marine habitats is discussed in Section 2.1.

Three areas in which *Pinna nobilis* are found nearby are (Tahht-il-Maqjel, Ras il Friek, Ras-il-Qali). These areas are shown in Drawing 1. Of these two (Ras il Friek and Ras il Qali) are found at the mouth of il Hofra iz Zghira bay.

### 5.2 Ecological Effects of Warm Water Discharge

A comprehensive review of the potential effects of the increased warm water discharge on the ecology of the receiving waters is outside the scope of this project and would require detailed ecological information about the fauna and flora of il Hofra iz Zghira bay.

However, one of the concerns raised is the potential effect on local populations of the Noble Pen Shell, *Pinna nobilis*. *P. nobilis* is listed as endangered under the 1992 European Council Directive on the conservation of natural habitats and wild fauna and flora (92/43/EEC, Annex IV). It has been protected by the Protocol for Specially Protected Areas Biological Diversity in the Mediterranean (Barcelona Convention: UNEP).

*P. nobilis* is the largest mollusc endemic to the Mediterranean Sea with a shell up to one meter in length. However it is vulnerable to damage and pollution. *Pinna nobilis* occurs in coastal areas at depths down to 60 m, often in soft-sediment areas overgrown by meadows of the seagrasses (e.g. *Posidonia oceanica*), but may also occur in rocky environments and even wrecks<sup>6</sup>. The species is long lived with sporadic local recruitment and highly variable numbers of recruits. The population has substantially declined over the past 30 years caused primarily by fishing and incidental killing by trawling and anchoring.

*P. nobilis* is reported<sup>7</sup> to grow in waters with temperatures up to 29.3°C. Katsanevakis<sup>8</sup> reported that temperature for the growth and reproduction of *P. nobilis* was relatively constant in Marine Lake Vouliagmeni, in Greece (annual temperature range of 11 to 29°C at depth <15m). Temperatures of 33-34 °C are reported to be lethal to *P. nobilis*.

The results of the modelling show that the areas of seabed that are likely to be most affected by the temperature plume occur in the very shallow areas on the west and northern shores of the bay. In these areas the water temperature may increase by 3°C under the worst conditions (this equates to 30°C at the height of summer). At the mouth of the bay the model predicts that the temperatures will only be increased in a very small area by a maximum of 1.5°C above ambient in the summer under conditions of strong winds (Section 4.1.2). This equates to a maximum summer temperature of 28.5°C.

Information into the effects of increased temperature on the survival of *Pinna nobilis* is scarce, but it is known that growth is generally ceases over the cold winter months and also

---

<sup>6</sup> Malta Environment and Planning Authority (2006). Protocol to study and monitor *Pinna nobilis* populations within Marine Protected Areas. (<http://www.mepa.org.mt>)

<sup>7</sup> Lotfi Rabaoui, Sabiha Tlig-Zouari, Stelios Katsanevakis Oum Kalthoum Ben Hassine. Modelling Population Density of *Pinna Nobilis* (Bivalvia) on the Eastern And Southeastern Coast of Tunisia

<sup>8</sup> Katsanevakis S: Population ecology of the endangered fan mussel *Pinna nobilis* in a marine lake. *Endangered Species Res*, 1, 1-9, 2005

slows at the height of the summer<sup>9</sup>. The slow growth in the summer occurred at temperatures of 29°C. It can therefore be concluded that the increased flow would not affect populations of the noble pen shell living on or outside the mouth of the bay since all seabed temperatures would be below this level. The increased water temperature over the winter might actually result in a slightly longer growing season.

It is not thought that there are populations of the noble pen shell in the bay itself (although to be certain this would need to be confirmed by targeted surveys). However, since the noble pen shell were still growing at 29°C in the study referred to above, it is highly unlikely that an extra degree of water temperature over a short period of time would affect the survival of these organisms. It is therefore thought that the increased seabed temperatures experienced within the majority of the bay would not prevent the noble pen shell from inhabiting these areas.

Some authors have postulated that an increase in water temperatures may result in reduced recruitment<sup>10</sup>, but no studies have been carried out in this species to support these views and there is no data that defines temperature maxima for either recruitment or the survival of the embryos in the plankton.

The reproduction of this endemic bivalve is concentrated between the months of March and September<sup>11</sup>, but is highly variable from year to year and location to location. It is not known exactly when populations of *Pinna nobilis* spawn in this area of Malta, but unless it occurs over the summer temperature maxima in August (as has been shown in some populations), it is thought very unlikely that this will be affected by the very small increase in water temperatures experienced as a result of the increased flow from the power station. Even if spawning/recruitment does occur over this period, there is no data to support or refute the theory that there may be a negative impact as more studies are required to determine this.

---

<sup>9</sup> Katsanevakis S (2007). Growth and mortality rates of the fan mussel *Pinna nobilis* in Lake Vouliagmani (Korinthiakos Gulf Greece): a generalized additive modelling approach. *Marine Biology* 152, 6, 1319 – 13331.

<sup>10</sup> Cabanellas-Reboredo M, Deudero S, Alos J, Valencia J M, March D, Hendricks I E and Alvarez E (2009). Recruitment of *Pinna nobilis* (Mollusca: Bivalvia) on artificial structures. *Marine Biodiversity Records* Vol 2:e126.

<sup>11</sup> Vicente N. (2003) Le grande nacre de Me'diterrane'e *Pinna nobilis*. *Me'mories de l'Institut Oce'anographique Paul Ricard*, pp. 7–16.



## 6.0 CONCLUSIONS

The effects of tide, general Mediterranean Sea circulation and seiches have been considered in this study of the Delimara power station (DPS) cooling water discharge. The study aims to predict the spread of the cooling water plume from the power station discharge into the adjacent bay, il Hofra iz Zghira. The study has considered the effect of the existing discharge flow rate of 29,500 m<sup>3</sup>/h and for an increased flow rate to 43,000 m<sup>3</sup>/h, both with a temperature 8°C above ambient temperature of the coastal waters.

Results show that the natural water flows in the area are low and that the flow dynamics in into il Hofra iz Zghira are dominated by the discharge. Predicted temperature contours have the same characteristics in winter and summer, but the summer temperatures are naturally approximately 12°C higher than the winter temperatures.

Predicted results are most easily described in terms of temperature increase above the background level of the coastal waters:

### Existing discharge rate:

- Surface temperature in the coastal waters (i.e. outside of il Hofra iz Zghira bay) are up to 1.5°C above background, and the temperature at the mouth of the bay is +2°C. Within the bay temperatures increase to +8°C at the outfall with the highest temperatures along the west and north coasts.
- Sea bed temperatures outside the bay are unaffected by the discharge. Within the bay sea bed temperatures are increased along the western and northern shores.
- Under conditions of strong winds and wave action the vertical mixing in the area is increased resulting in warmer water being mixed to the sea bed. Water of +0.5°C is predicted to occur at the bed in limited areas outside the bay; the sea bed temperature at the southern point of the mouth of the bay is +1°C, which would give a maximum of 28°C at the height of the summer.

### Increased discharge rate:

- Surface temperature in the coastal waters (i.e. outside of il Hofra iz Zghira bay) are up to 2°C above background, and the temperature at the mouth of the bay on the northern side is +3°C. Within the bay temperatures increase to +8°C at the outfall with the highest temperatures along the west and north coasts.
- Sea bed temperatures outside the bay are unaffected by the discharge. Within the bay sea bed temperatures are increased along the western and northern shores.
- Under conditions of strong winds and wave action the vertical mixing in the area is increased resulting in warmer water being mixed to the sea bed. Water of +1°C is predicted to occur at the bed in limited areas outside the bay, and the sea bed temperature at the southern point of the mouth of the bay is +1.5°C in a very small area, which would give a maximum of 28.5°C at the height of the summer.

Cooling water from the existing DPS discharge or from an increase in capacity is highly unlikely to have an effect on known populations or habitats of sensitive or protected sea bed species including the noble pen shell, *Pinna nobilis*.

## **7.0 CLOSURE**

This report has been prepared by SLR Consulting Limited with all reasonable skill, care and diligence, and taking account of the manpower and resources devoted to it by agreement with the client. Information reported herein is based on the interpretation of data collected and has been accepted in good faith as being accurate and valid.

This report is for the exclusive use of AIS; no warranties or guarantees are expressed or should be inferred by any third parties.

SLR disclaims any responsibility to the client and others in respect of any matters outside the agreed scope of the work.

### Drawing 1 Environmentally Sensitive Areas



### APPENDIX A FVCOM MODEL

The model is called FVCOM (Finite Volume Coastal Ocean Model) created at the Marine Ecosystem Dynamics Modelling Laboratory in the School of Marine Science and Technology at the University of Massachusetts-Dartmouth. FVCOM is a 3-dimensional hydrodynamic model to compute tidal flows in an estuary, a coastal region or in the open ocean. In this study FVCOM has been applied to the central Mediterranean Sea, with particular focus on the Maltese islands. (<http://fvcom.smast.umassd.edu/FVCOM/index.html>).

FVCOM includes a “particle tracking” routine, and this has been enhanced to compute the movement and dilution of effluents discharged from a marine outfall.

This extract from the FVCOM User's Manual (Chen *et al.*, 2006) gives information on the development of the model and on the scope of the model:

“FVCOM is a prognostic, unstructured-grid, finite-volume, free-surface, three-dimensional (3-D) primitive equations ocean model developed originally by Chen *et al.* (2003a). The original version of FVCOM consists of momentum, continuity, temperature, salinity and density equations and is closed physically and mathematically using the Mellor and Yamada level 2.5 turbulent closure scheme for vertical mixing and the Smagorinsky turbulent closure scheme for horizontal mixing. The irregular bottom topography is represented using the  $\sigma$ -coordinate transformation, and the horizontal grids are comprised of unstructured triangular cells. FVCOM solves the governing equations in integral form by computing fluxes between non-overlapping horizontal triangular control volumes. This finite-volume approach combines the best of finite element methods (FEM) for geometric flexibility and finite-difference methods (FDM) for simple discrete structures and computational efficiency. The numerical approach also provides a much better representation of mass, momentum, salt, and heat conservation in coastal and estuarine regions with complex geometry. The conservative nature of FVCOM in addition to its flexible grid topology and code simplicity make FVCOM ideally suited for application in the coastal ocean.

The initial development of FVCOM was started by a team effort led by C. Chen in 1999 at the University of Georgia with support from the Georgia Sea Grant College Program. This first version was designed to simulate the 3-D currents and transport within an estuary/tidal creek/inter-tidal salt marsh complex and was written in Fortran 77 in 2001. In 2001, C. Chen moved to the School of Marine Science and Technology at the University of Massachusetts-Dartmouth (SMAS/UMASS-D) and established the Marine Ecosystem Dynamics Modeling (MEDM) Laboratory where work on FVCOM has continued with funding from several sources including the NASA and NOAA-funded SMAS/UMASS fishery program led by Brian Rothschild, the NSF/NOAA US GLOBEC/Georges Bank Program. The scientific team led by C. Chen and R. C. Beardsley (Woods Hole Oceanographic Institution-WHOI) built the original structure of FVCOM and conducted a series of model validation experiments. G. Cowles joined the MEDM group in 2003 and lead the conversion of FVCOM to Fortran 90/95, modularized the coding structure, and added the capability for parallel computation. The original version of FVCOM included a nudging data assimilation module added by H. Liu, an improved 3-D wet/dry point treatment module modified and tested by J. Qi, several choices for freshwater discharge and groundwater input and turbulence modules by C. Chen, H. Liu and G. Cowles, a tracer-tracking module by Q. Xu, a 3-D Lagrangian particle tracking code (originally written by C. Chen and L. Zheng, modified by H. Liu to fit FVCOM, and corrected by G. Cowles), several types of companion finite-volume biological models such as a) a nutrient-phytoplankton-zooplankton (NPZ) model developed by Franks and Chen (1996; 2001) an 8-component phosphorus limited, lower trophic level food web model (nutrients, two sizes of phytoplankton, two sizes of zooplankton, detritus and bacteria:



## APPENDIX A

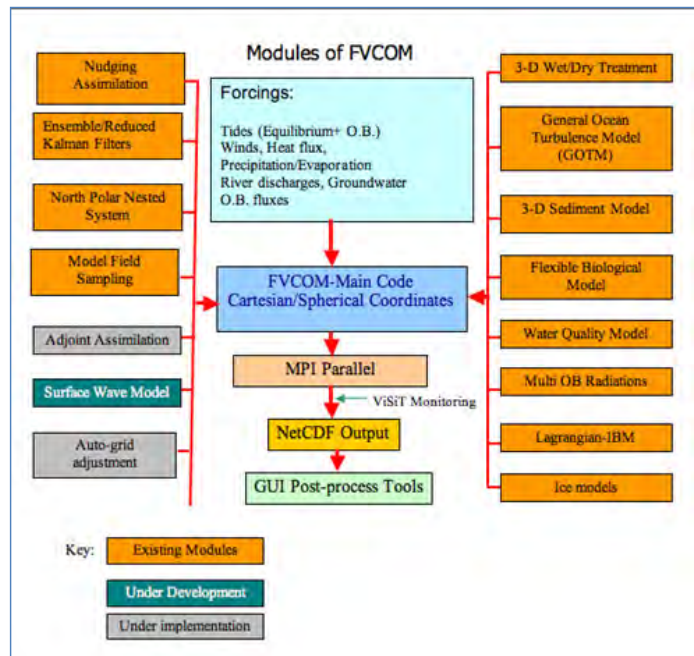
### THERMAL MODELLING REPORT

NPZDB) developed by Chen et al. (2002)) a state-of the art water quality model with inclusion of the benthic flux developed by Zheng and Chen (Zheng et al. 2004)) a 9-component coastal ocean NPZD model developed by R. Ji and C. Chen (Ji, 2003)) a simple tracer-based 3-D sediment model developed by L. Zheng and C. Chen (Zheng et al., 2003).

FVCOM has been significantly upgraded since the workshop held in June 2005 at SMAST. The present version of FVCOM includes many new options and components. The code has been extended for optional solution in a spherical-coordinate system with multiple choices of the turbulence parameterization through the General Ocean Turbulent Model (GOTM) modules (Burchard, 2002), 4-D nudging and Reduced/Ensemble Kalman Filters (implemented in collaboration with P. Rizzoli) for data assimilation, a fully-nonlinear ice model (implemented by F. Dupont) for Arctic Ocean studies, a 3-D sediment transport module (developed by G. Cowles based on the U.S.G.S. community sediment transport model) for estuarine and near-shore applications, and a generalized biological module (GBM) (developed by C. Chen, R. Tian, J. Qi and R. Ji) for food web dynamics studies, etc. Multiple open boundary conditions have also been added to the code (done by H. Huang, C. Chen and J. Qi) for the purpose of radiating energy out of the computational domain and adding the low frequency mass flux.

As the FVCOM development team leader, Changsheng Chen reserves all rights of this product. The University of Massachusetts-Dartmouth owns the copyright of the software of this model. All copyrights are reserved. Unauthorized reproduction and distribution of this program are expressly prohibited. This program is only permitted for use in non-commercial academic research and education. The commercial use is subject to a fee. Contributions made to correcting and modifying the program will be credited, but not affect copyrights."

#### Flow Diagram of the FVCOM Model:



For the present estuary study the following modules are not included in the model:

- General Ocean Turbulence model
- 3-D sediment model
- Biological model
- Water Quality model
- Ice models
- Nudging assimilation
- Kalman filters
- North Polar nested system
- MPI parallel code

Modelling was refined and undertaken by Ecospan 2011. The following extract from the User's Manual shows the theoretical equations that are solved by FVCOM:

### The Model Formulation: The Primitive Equations in Cartesian Coordinates

The governing equations consist of the following momentum, continuity, temperature, salinity, and density equations:

$$\frac{\partial u}{\partial t} + u \frac{\partial u}{\partial x} + v \frac{\partial u}{\partial y} + w \frac{\partial u}{\partial z} - f v = -\frac{1}{\rho_0} \frac{\partial P}{\partial x} + \frac{\partial}{\partial z} \left( K_v \frac{\partial u}{\partial z} \right) + F_u \quad (2.1)$$

$$\frac{\partial v}{\partial t} + u \frac{\partial v}{\partial x} + v \frac{\partial v}{\partial y} + w \frac{\partial v}{\partial z} + f u = -\frac{1}{\rho_0} \frac{\partial P}{\partial y} + \frac{\partial}{\partial z} \left( K_v \frac{\partial v}{\partial z} \right) + F_v \quad (2.2)$$

$$\frac{\partial P}{\partial z} = -\rho g \quad (2.3)$$

$$\frac{\partial u}{\partial x} + \frac{\partial v}{\partial y} + \frac{\partial w}{\partial z} = 0 \quad (2.4)$$

$$\frac{\partial T}{\partial t} + u \frac{\partial T}{\partial x} + v \frac{\partial T}{\partial y} + w \frac{\partial T}{\partial z} = \frac{\partial}{\partial z} \left( K_t \frac{\partial T}{\partial z} \right) + F_T \quad (2.5)$$

$$\frac{\partial S}{\partial t} + u \frac{\partial S}{\partial x} + v \frac{\partial S}{\partial y} + w \frac{\partial S}{\partial z} = \frac{\partial}{\partial z} \left( K_s \frac{\partial S}{\partial z} \right) + F_S \quad (2.6)$$

$$\rho = \rho(T, S) \quad (2.7)$$

where  $x$ ,  $y$ , and  $z$  are the east, north, and vertical axes in the Cartesian coordinate system,  $u$ ,  $v$ , and  $w$  are the  $x$ ,  $y$ ,  $z$  velocity components;  $T$  is the temperature;  $S$  is the salinity;  $\rho$  is the density;  $P$  is the pressure;  $f$  is the Coriolis parameter;  $g$  is the gravitational acceleration;  $K_v$  is the vertical eddy viscosity coefficient; and  $K_t$  is the thermal vertical eddy

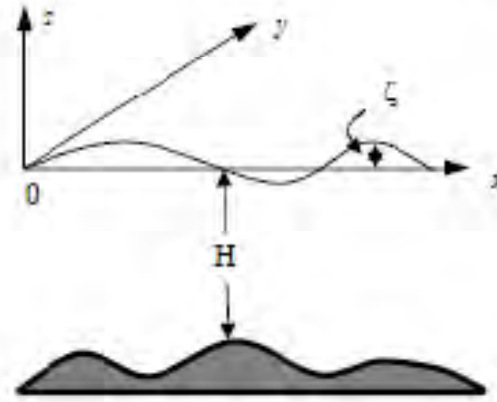


Fig. 2.1: Illustration of the orthogonal coordinate system:  $x$ : eastward;  $y$ : northward;  $z$ : upward

diffusion coefficient.  $F_u$ ,  $F_v$ ,  $F_T$ , and  $F_S$  represent the horizontal momentum, thermal, and salt diffusion terms. The total water column depth is  $D = H + \zeta$ , where  $H$  is the bottom depth (relative to  $z = 0$ ) and  $\zeta$  is the height of the free surface (relative to  $z = 0$ ).

## References

- Burchard H, 2001. Simulating the wave-enhanced layer under breaking surface waves with two-equation turbulence models. *J. Phys. Oceanogr.*, 31, 3133-3145.
- Burchard H, 2002. Applied turbulence modeling in marine waters. *Springer:Berlin-Heidelberg-New York-Barcelona-Hong Kong-London-Milan Paris-Tokyo*, 215pp.
- Burchard H, Baumert H, 1995. On the performance of a mixed-layer model based on the  $k-\varepsilon$  turbulence closure. *J. Geophys. Res.*, 100 (C5), 8523-8540.
- Chen C, Ji R, Schwab D, Beletsky D, Fahnenstiel D, Jiang M, Johengen T H, Lavrentyev H, Eadie B, Budd J W, Bundy M, Gardner W, Cotner J, Lavrentyev P J, 2002. A coupled biological and physical model study of the ecosystem in Lake Michigan Part I: A 1-D experiment. *Ecological Modeling*, 152, 145-168.
- Chen C, Liu H, R C Beardsley R C, 2003. An unstructured, finite-volume, three-dimensional, primitive equation ocean model: application to coastal ocean and estuaries. *J. Atm.&Oceanic Tech.*, 20, 159-186.
- Chen C, Robert C. Beardsley R C, Cowles G, 2006. An Unstructured Grid, Finite-Volume Coastal Ocean Model FVCOM: Users Manual.
- Dyer K R, 1990. Tidally generated estuarine mixing processes. Hydrodynamics of estuaries, Volume 1: estuarine processes, edited by Kjerfve B, 41-57.
- Franks P J S, Chen C, 1996. Plankton production in tidal fronts: a model of Georges Bank in summer. *J. Mar. Res.*, 54, 631-651.
- Franks P J S, Chen C, 2001. A 3-D prognostic numerical model study of the Georges Bank ecosystem. Part II: biological-physical model. *Deep Sea Res. II*, 48, 457-482.
- Ji R, 2003. Biological and physical processes controlling the spring phytoplankton bloom dynamics on Georges Bank. Ph.D. Thesis. The University of Georgia, 216pp.
- Zheng L, Chen C, Alber M, Liu H, 2003. A modeling study of the Satilla River Estuary, Georgia. II: Suspended sediment. *Estuaries*, 26(3), 670-679.
- Zheng L, Chen C, Zhang F, 2004. Development of water quality model in the Satilla River estuary, Georgia. *Ecological Modeling*, 178, 457-482.
- Riddle A M, Lewis R E, (2000). Dispersion experiments in UK coastal waters. *Estuarine, Coastal and Shelf Science*, 51, 243-254.
- ECOSPAN 2011. Report to SLR Consulting. Ref R11-146: Prediction of the spread and dilution of the cooling water plume from the Delimara power station, east Malta.





global environmental solutions

**AYLESBURY**

7 Wornal Park, Menmarsh Road,  
Worminghall, Aylesbury,  
Buckinghamshire HP18 9PH  
T: +44 (0)1844 337380

**BELFAST**

24 Ballynahinch Street, Hillsborough,  
Co. Down, BT26 6AW Northern Ireland  
T: +44 (0)28 9268 9036

**BRADFORD-ON-AVON**

Treenwood House, Rowden Lane,  
Bradford-on-Avon, Wiltshire BA15 2AU  
T: +44 (0)1225 309400

**BRISTOL**

Langford Lodge, 109 Pembroke Road,  
Clifton, Bristol BS8 3EU  
T: +44 (0)117 9064280

**CAMBRIDGE**

8 Stow Court, Stow-cum-Quy, Cambridge  
CB25 9AS  
T: + 44 (0)1223 813805

**CARDIFF**

Fulmar House, Beignon Close, Ocean  
Way, Cardiff CF24 5HF  
T: +44 (0)29 20491010

**CHELMSFORD**

Unit 77, Waterhouse Business Centre,  
2 Cromar Way, Chelmsford, Essex  
CM1 2QE  
T: +44 (0)1245 392170

**DUBLIN**

7 Dundrum Business Park, Windy  
Arbour, Dundrum, Dublin 14 Ireland  
T: + 353 (0)1 2964667

**EDINBURGH**

No. 4 The Roundal, Roddinglaw  
Business Park, Gogar, Edinburgh  
EH12 9DB  
T: +44 (0)131 3356830

**EXETER**

69 Polsloe Road, Exeter EX1 2NF  
T: + 44 (0)1392 490152

**FARNBOROUGH**

The Pavilion, 2 Sherborne Road, South  
Farnborough, Hampshire GU14 6JT  
T: +44 (0)1252 515682

**GLASGOW**

4 Woodside Place, Charing Cross,  
Glasgow G3 7QF  
T: +44 (0)141 3535037

**HUDDERSFIELD**

Westleigh House, Wakefield Road,  
Denby Dale, Huddersfield HD8 8QJ  
T: +44 (0)1484 860521

**LEEDS**

Suite 1, Jason House, Kerry Hill,  
Horsforth, Leeds LS18 4JR  
T: +44 (0)113 2580650

**MAIDSTONE**

19 Hollingworth Court, Turkey Mill,  
Maidstone, Kent ME14 5PP  
T: +44 (0)1622 609242

**NEWCASTLE UPON TYNE**

Sailors Bethel, Horatio Street,  
Newcastle-upon-Tyne NE1 2PE  
T: +44 (0)191 2611966

**NOTTINGHAM**

Aspect House, Aspect Business Park,  
Bennerley Road, Nottingham NG6 8WR  
T: +44 (0)115 9647280

**ST. ALBAN'S**

White House Farm Barns, Gaddesden  
Row, Hertfordshire HP2 6HG  
T: +44 (0)1582 840471

**SHEFFIELD**

STEP Business Centre, Wortley Road,  
Deepcar, Sheffield S36 2UH  
T: +44 (0)114 2903628

**SHREWSBURY**

Mytton Mill, Forton Heath, Montford  
Bridge, Shrewsbury SY4 1HA  
T: +44 (0)1743 850170

**STAFFORD**

8 Parker Court, Staffordshire Technology  
Park, Beaconside, Stafford ST18 0WP  
T: +44 (0)1785 253331

**WARRINGTON**

Suite 9 Beech House, Padgate Business  
Park, Green Lane, Warrington WA1 4JN  
T: +44 (0)1925 827218

**WORCESTER**

Suite 5, Brindley Court, Gresley Road,  
Shire Business Park, Worcester  
WR4 9FD  
T: +44 (0)1905 751310



Energy



Waste  
Management



Planning &  
Development



Industry



Mining  
& Minerals



Infrastructure